HydroFATE (v1): A high-resolution contaminant fate model for the global river system

Heloisa Ehalt Macedo[1], Bernhard Lehner[1], Jim Nicell[2], Günther Grill[1]

5   [1]Department of Geography, McGill University, Montreal, QC H3A 0B9, Canada
[2]Department of Civil Engineering, McGill University, Montreal, QC H3A 0C3, Canada

Correspondence to: Heloisa Ehalt Macedo (heloisa.ehaltmacedo@mail.mcgill.ca) and Bernhard Lehner (bernhard.lehner@mcgill.ca)

10   **Abstract.** Pharmaceuticals and household chemicals are neither fully consumed nor fully metabolized when routinely used by humans, thereby resulting in the emission of residues down household drains and into wastewater collection systems. Since treatment systems cannot entirely remove these substances from wastewaters, the contaminants from many households connected to sewer systems are continually released into surface waters. Furthermore, diffuse contributions of wastewaters from populations that are not connected to treatment systems can directly (i.e., through surface runoff) or indirectly (i.e., through soils and groundwater) contribute to contaminant concentrations in rivers and lakes. The unplanned and unmonitored release of such contaminants can pose important risks to aquatic ecosystems and ultimately human health. In this work, the contaminant fate model HydroFATE is presented which is designed to estimate the surface-water concentrations of domestically used substances for virtually any river in the world. The emission of compounds is calculated based on per capita consumption rates and population density. A global database of wastewater treatment plants is used to separate the effluent pathways from populations into treated and untreated, and to incorporate the contaminant pathways into the river network. The transport in the river system is simulated while accounting for processes of environmental decay in streams and in lakes. To serve as a preliminary performance evaluation and proof of concept of the model, the antibiotic sulfamethoxazole (SMX) was chosen, due to its widespread use and the availability of input and validation data. The comparison of modelled concentrations against a compilation of reported SMX measurements in surface waters revealed reasonable results despite inherent model uncertainties. A total of 390,000 km of rivers were predicted to have SMX concentrations that exceed environmental risk thresholds. Given the high spatial resolution of predictions, HydroFATE is particularly useful as a screening tool to identify areas of potentially elevated contaminant exposure and to guide where local monitoring and mitigation strategies should be prioritized.

1 Introduction

30   Compounds of emerging concern (CECs) are deemed to be an important source of risk due to their potential adverse environmental impacts in the global water system (Gavrilescu et al., 2015; Noguera-Oviedo & Aga, 2016). For instance, pharmaceutically active compounds such as analgesics, antibiotics, estrogens and antiepileptics which are in widespread use globally, are not fully metabolized by the human body; thus, after their excretion and subsequent delivery into the wastewater collection and treatment system, they may ultimately reach the aquatic environment (Aydin et al., 2019; Kümmerer, 2009;

35   Palli et al., 2019; Patrolecco et al., 2018; Praveena et al., 2018). The ongoing release of these compounds and other household chemicals through wastewater discharges often has unknown or poorly understood effects on the environment and human health. Importantly, most wastewater treatment plants (WWTPs) are not specifically designed to remove these contaminants before discharging effluents into receiving waterbodies, such as rivers, lakes, or oceans (Rizzo et al., 2019). As such, wastewaters that are collected from domestic sources and delivered via sewer systems to a WWTP may be only partially – or

40   not at all – treated for such substances, thereby causing the WWTP to serve as a concentrated point source of contamination of CECs into aquatic ecosystems (Daughton & Ternes, 1999; Petrie et al., 2015; Meyer et al., 2019). In addition to these point sources, diffuse sources of contaminants from populations who are not connected to the sewage system can add to the pollution of waterbodies (Lapworth et al., 2012). Risks associated with these contaminants are further exacerbated due to the limited monitoring of their presence in wastewaters and receiving waterbodies into which they are discharged, and incomplete

45   assessment of their impacts downstream. In turn, this lack of information leads to poor regulatory oversight to safeguard the health of aquatic ecosystems and that of populations that rely on them as a source of water (Daughton, 2014). Moreover, robust estimates of current and future changes in water quality are needed to achieve sustainable management of water resources to ensure clean and accessible water for all, as promoted by the Sustainable Development Goal (SDG) 6 (Strokal et al., 2019; Tang et al., 2019; van Vliet et al., 2019).

50   When measurements of waterborne contaminants are unavailable or insufficient to make informed decisions regarding water pollution arising from CECs, simulation models can be used instead to represent the hydrodynamic and water quality conditions of the waterbody. Contaminant fate models (CFMs), also known as environmental exposure models or georeferenced river models, focus on instream processes such as transport and degradation after the compounds' release from point and non-point sources. CFMs are specifically designed to predict realistic distributions of contaminants in a river

55   catchment (Aldekoa et al., 2016). Examples of models operating at regional to global scales include GREAT-ER (Aldekoa et al., 2013; Feijtel et al., 1997), LF2000-WQX (Johnson et al., 2007), GIS-ROUT (Wang et al., 2000), PhATE (Anderson et al., 2004), Mike 11 (Havnø et al., 1995), WorldQual (Voß et al., 2012), ePiE (Oldenkamp et al., 2018), and GWAVA (Johnson et al., 2013). These models require information about the hydrological characteristics of the catchment, consumption rates of the chemical substances, and fate parameters that describe their instream decay. These requirements can limit the performance of

60   the models in regions where this information is unreliable or scarce (Grill et al., 2016).

Water pollution caused by CECs is an issue of global concern, and water quality assessments must therefore be spatially consistent and comparable across the world to be able to identify locations of high contaminant concentration and regional trends in water pollution over time at a global scale. One of the challenges for global contaminant fate modelling is the lack of spatial consistency in datasets for model inputs, especially in regions where data are insufficient to support detailed

65 assessments. (Kroeze et al., 2016; Strokal et al., 2019; Tang et al., 2019). For this reason, only a few global-scale CFMs models exist, and those that do are typically limited to certain substances and relatively coarse spatial resolutions. For example, GLOBAL-FATE (Font et al., 2019), which was created as an open-source down-the-drain model that includes lake and reservoir modules as well as wastewater input information at a global scale, operates at a 7-km spatial grid. The Global TCS model (van Wijnen et al., 2018) was created to simulate the transport of the antibacterial agent triclosan in global rivers at a

70 0.5-degree spatial resolution (i.e., corresponding to approximately 55-km grid cells at the equator).

To our knowledge, all currently existing global CFMs that require the quantification of the load of wastewater into the river system use population density and national sanitation statistics as proxies to derive the necessary input data (e.g., Beusen et al., 2015; Font et al., 2019; Hofstra et al., 2013; Mayorga et al., 2010; Strokal et al., 2019; Van Drecht et al., 2009; van Puijenbroek et al., 2019; Williams et al., 2012). More specifically, calculations are based on the fraction of the population

75 connected to sewage systems per country. The main source of these statistics is the World Health Organization and the United Nation Children's Fund (WHO/UNICEF) Joint Monitoring Program (JMP) for Water Supply, Sanitation and Hygiene (WASH), which provides regular global reports on drinking-water and sanitation coverage for tracking progress toward SDG 6 (WHO & UNICEF, 2021). This dataset allows for differentiation of wastewater treatment services between countries and over time, but it does not account for spatial variability inside national boundaries, except for an assumed correlation with

80 population density. Herrera (2019) also points out several discrepancies between national-level data and JMP-WASH data. In addition, the dataset does not contain specific locations of wastewater discharge, which can have important implications with respect to the distribution of contaminants in the river system.

Another important limitation of existing global water quality models is that they do not account for diffuse sources of pollution arising from populations who are not connected to WWTPs or for the natural attenuation of contaminants that occurs along

85 their pathway from a source in the landscape through the soil or subsurface before reaching a waterbody. The contribution of diffuse pollution can be substantial as revealed by the high aquatic concentrations of pharmaceuticals that have been measured in countries with low rates of sanitation (Hanna et al., 2020; K'Oreje et al., 2012; Khan et al., 2013).

Grill et al. (2016; 2018) introduced a regional CFM that estimates the emission of household contaminants and their subsequent transport in river networks at high spatial resolution (river network derived from 500-m grid cells). In this model, transport in

90 the river system is simulated using the global river routing model HydroROUT (Lehner & Grill, 2013). It has been applied and evaluated with respect to its ability to model the fate of several pharmaceuticals in the Saint Lawrence River Basin, Canada (Grill et al., 2016), the pharmaceutical diclofenac in India (Shakya, 2017), and human hormones in China (Grill et al., 2018). These assessments included not only WWTPs as point sources but also accounted for diffuse sources of contamination from populations not served by WWTPs while accounting for natural attenuation.

95   In the present work, the CFM by Grill et al. (2016; 2018) is fully developed to operate at a global scale in order to: (1) serve as a large-scale screening tool for assessing CECs from domestic sources, especially as a precursor for potential risk assessments; (2) predict critical locations in river networks of potentially high aquatic contaminations; and (3) inform the development and implementation of guidelines, regulations and mitigation strategies that aim to limit chemical pollution and safeguard human and ecosystem health. The model enhancement and expansion are performed by integrating a global WWTP

100   database (HydroWASTE; Ehalt Macedo et al., 2022) and by distinguishing the pathways of contaminants from their population source to the river network depending on whether they are treated (i.e., either in centralized WWTPs or in decentralized facilities) or untreated (i.e., either from urban or rural diffuse sources). The capability of this global model, hereafter called HydroFATE, is then evaluated by applying it to estimate the global distribution of the antibiotic sulfamethoxazole (SMX) in the river network and by then comparing the resulting predictions of environmental concentrations to field measurements

105   reported in the literature. SMX was selected for this proof-of-concept case study due to the abundance of SMX field measurements in surface waters reported globally and the broader availability of model input parameters in the literature compared to many other CECs.

Given the broad goals, the main focus of the model development presented herein is to predict spatial variations in contaminant exposure and to achieve a level of model performance where estimates of concentrations in the river network are generally

110   within an order-of-magnitude of reported field measurements, which is generally considered adequate for these types of screening models (Johnson et al., 2008, Oldenkamp et al., 2018). HydroFATE, with its inherent global applicability due to its reliance on pre-existing data in addition to its high spatial resolution, aims to provide a tool for scientists, practitioners, and regulators to advance and focus their work, especially in regions where data are lacking.

2 Data

115   ### 2.1 River and lake network

The various raster and vector layers representing the river network and catchment boundaries in HydroFATE were obtained from the global hydrographic database HydroSHEDS (Lehner et al., 2008), which was derived from digital elevation data provided by NASA's Shuttle Radar Topography Mission (SRTM) at 90 m (3 arcsecond) resolution. For the present study, we used a derivative of this database in vector format, termed RiverATLAS (Linke et al., 2019), which was extracted at 500 m

120   (15 arcsecond) grid cell resolution and represents all rivers and streams where the average discharge exceeds 100 L s^{-1} or the upstream catchment area exceeds 10 km^2, or both. The resulting global river network comprises 8,477,883 individual river reaches with an average length of 4.2 km, representing a total of 35.8 million kilometers of rivers. Each river reach has an associated contributing catchment with an average area of 15.7 km^2.

Every river reach in RiverATLAS is provided with a series of precalculated hydro-environmental characteristics. From this

125   database, we used the long-term (i.e., 1971 to 2000) average naturalized river discharge in our study. The discharge estimates were derived from the global hydrological model WaterGAP version 2.2 (Müller Schmied et al., 2014), which were downscaled

from their original resolution of 0.5° grid cells to the RiverATLAS resolution of 500 m using geostatistical techniques (Lehner & Grill, 2013). In addition to annual average discharge estimates, minimum discharges (i.e., the lowest monthly flow value within an average year) were also used for assessments under low-flow conditions.

130 To account for lake processes, a global database called HydroLAKES was used that provides the shoreline polygons of 1.4 million lakes with a surface area of at least 10 ha (Messager et al., 2016). All lakes in HydroLAKES are associated with RiverATLAS via their lake pour points.

2.2 WWTP information

HydroFATE incorporates the locations and characteristics of wastewater treatment plants (WWTPs) as provided by the
135 HydroWASTE database (Ehalt Macedo et al., 2022). This database contains information on 58,502 WWTPs and provides details for each on the actual location of the plant, the estimated outfall location, and attributes that are relevant for the purposes of this study including: population served, treated-wastewater discharge, and level of treatment; i.e., primary treatment, such as solids removal through mechanical cleaning and sedimentation; secondary treatment, which includes biological processes; and advanced (tertiary or higher) treatment through extra filtration or chemical treatment. HydroWASTE was developed by
140 combining regional and national WWTP datasets and adding auxiliary information, including Open Street Map data, global population data, and the high-resolution river network from RiverATLAS which was used to georeference WWTP outfall locations.

With respect to its implementation in HydroFATE, of the 58,502 WWTPs in the database, the following were excluded (note that some records fall into more than one category): (1) 1,682 WWTPs that were labeled as *closed, non-operational,*
145 *decommissioned, projected, proposed,* or *under construction*; (2) 379 WWTPs that have their outfall location outside of any catchment that is associated with the river network of RiverATLAS (e.g., small islands); (3) 199 WWTPs that serve a population of zero according to records; and (4) 10,196 WWTPs that have their outfall location within 10 km from the ocean coast. The latter category was excluded to avoid overestimation of contaminant loads in coastal rivers as, given the locational uncertainties in HydroWASTE, effluents from WWTPs with estimated outfall locations near the coast might, in reality,
150 discharge directly into the ocean. Of the remaining 46,425 WWTPs, some share the same estimated outfall location, and thus were aggregated to the final number of 45,348 point sources of wastewater discharge into the global river network.

To account for small or decentralized wastewater treatment systems (DWTS) not included in the HydroWASTE database, such as septic tanks, HydroFATE uses country-level statistics provided by the JMP-WASH program (WHO & UNICEF, 2021). For the purposes of our study, sanitation data for each country were acquired for the year 2015 and the information termed
155 'Proportion of population using improved sanitation facilities (wastewater treated)' was selected.

2.3 Population and urban area grids

Global gridded population distributions of the year 2015 were provided by the WorldPop dataset (WorldPop & CIESIN, 2018), which was produced using a combination of census, geospatial, and remotely sensed data in a spatial modelling framework

(Tatem, 2017). The WorldPop data were disaggregated from their original spatial resolution of 1 km to the same resolution as

160   the HydroFATE model (500 m) to allow for spatially consistent calculations.

Information on the location of global urban areas is determined in HydroFATE according to a land use classification derived from remote sensing imagery. The dataset has a 500 m spatial resolution and is based on data from 2001 to 2002 from the Moderate Resolution Imaging Spectroradiometer (MODIS) (Schneider et al., 2010). Although more recent urban area grids exist today, this version was implemented during earlier model development stages and was kept to ensure model integrity.

165   **3 Methodology**

The regional CFM previously developed by Grill et al. (2016; 2018) simulates both the emission of household contaminants and their subsequent transport towards and within the river system. Building on this earlier work, we here enhance and then expand this CFM, hereafter termed HydroFATE, to the global scale. Figure 1 provides a conceptual representation of the HydroFATE model. Contaminant emissions are determined based on population distribution, per capita consumption of the

170   modelled substance, human metabolism, and wastewater treatment removal or natural attenuation, depending on the pathway from the source to the waterbody. Emissions from populations served by a WWTP or by smaller and decentralized wastewater treatment systems (DWTS) are reduced in proportion to the treatment efficiency, which is based on the level of treatment, i.e., primary, secondary, or advanced (tertiary or higher), that is provided by the WWTP. Emissions arising from populations that are not served by any type of wastewater treatment system are attenuated by a direct discharge coefficient depending on the

175   distance from the river network and whether the emission is located in a rural or urban area (Grill et al. 2018). The combined loads from all pathways of contaminants inside the catchment boundaries of an individual river reach are aggregated as the total local contaminant load of the reach. HydroFATE then employs the generic river routing model HydroROUT (Grill et al., 2014; 2019; Lehner & Grill, 2013) to simulate the transport of the chemical substance in the river system, accumulating the contaminant load downstream and accounting for instream decay and removal in lakes. Finally, the Predicted Environmental

180   Concentration (PEC) for every river reach is calculated by dividing the sum of the local total contaminant load plus the incoming load from upstream reaches by the long-term river discharge of the reach.
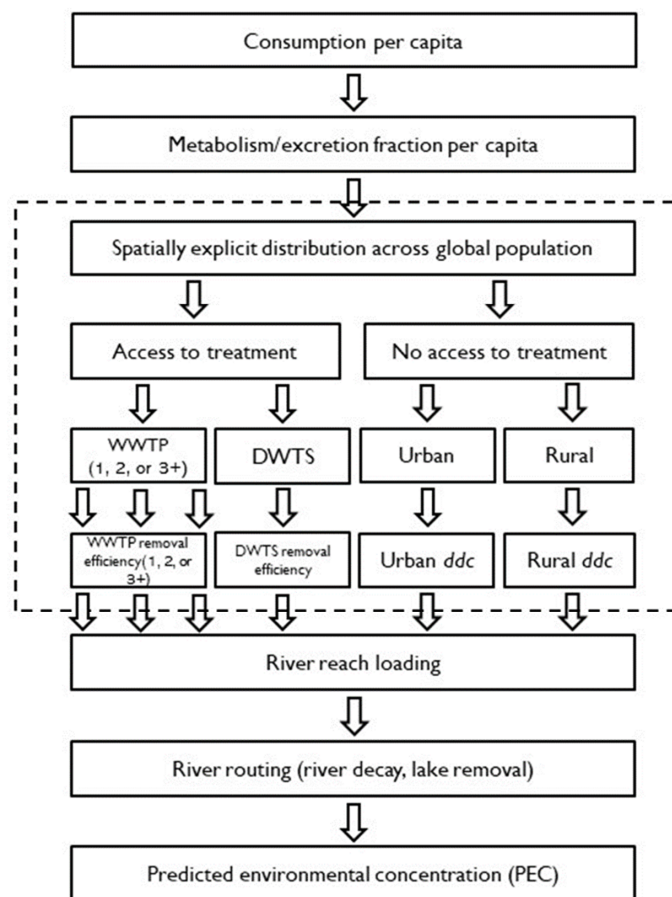
Figure 1. Conceptual representation of the contaminant fate model HydroFATE. The abbreviations '1, 2, or 3+' refer to the level of treatment of each WWTP as primary, secondary, or tertiary/advanced, respectively. The dotted rectangle highlights steps involving contaminant pathways, i.e., processes developed or enhanced in the present study. See text for details and model description. Modified from Grill et al. (2018).

The methodologies used to simulate the amount of contaminant emissions and the routing of contaminant loads along rivers and through lakes were previously described at the regional scale (Grill et al., 2016; 2018). While these basic processes do not change when applied at the global scale, the model was expanded in the present study by incorporating novel global-scale input data. Furthermore, the model was enhanced by introducing a spatially explicit differentiation of various wastewater and contaminant pathways depending on the access of global populations to wastewater treatment (see dotted rectangle in Figure 1). Within each pathway, contaminants are removed following different removal efficiencies offered by treatment facilities, or different levels of natural attenuation in the soil and subsurface.

3.1 Determination of contaminant pathways

195

HydroFATE calculates contaminant emissions using contaminant-specific information (i.e., the annual per capita consumption and the excretion fraction) and the number of people connected to the river system. This connection occurs through different pathways depending on the sanitation system at the location in question. Using the global WWTP database HydroWASTE (Ehalt Macedo et al., 2022), a population grid, an urban extent grid and additional sanitation data, six types of contaminant

200   pathways from populations into the river network were determined and incorporated into the HydroFATE model (see Figure 1). These are: point sources of treated wastewater from populations connected to WWTPs that provide (1) primary level of treatment, (2) secondary level of treatment, or (3) advanced (i.e., tertiary or higher) level of treatment; (4) decentralized sources of treated wastewater from populations not connected to a WWTP but served by DWTS; (5) diffuse sources of untreated wastewater from populations in urban areas; and (6) diffuse sources in rural areas. The methods described in more detail below

205   assign a contaminant pathway for every pixel in a global population grid. Figure 2 illustrates an example of the resulting pathway allocation in comparison to the population distribution at a metropolitan area and its rural surroundings.
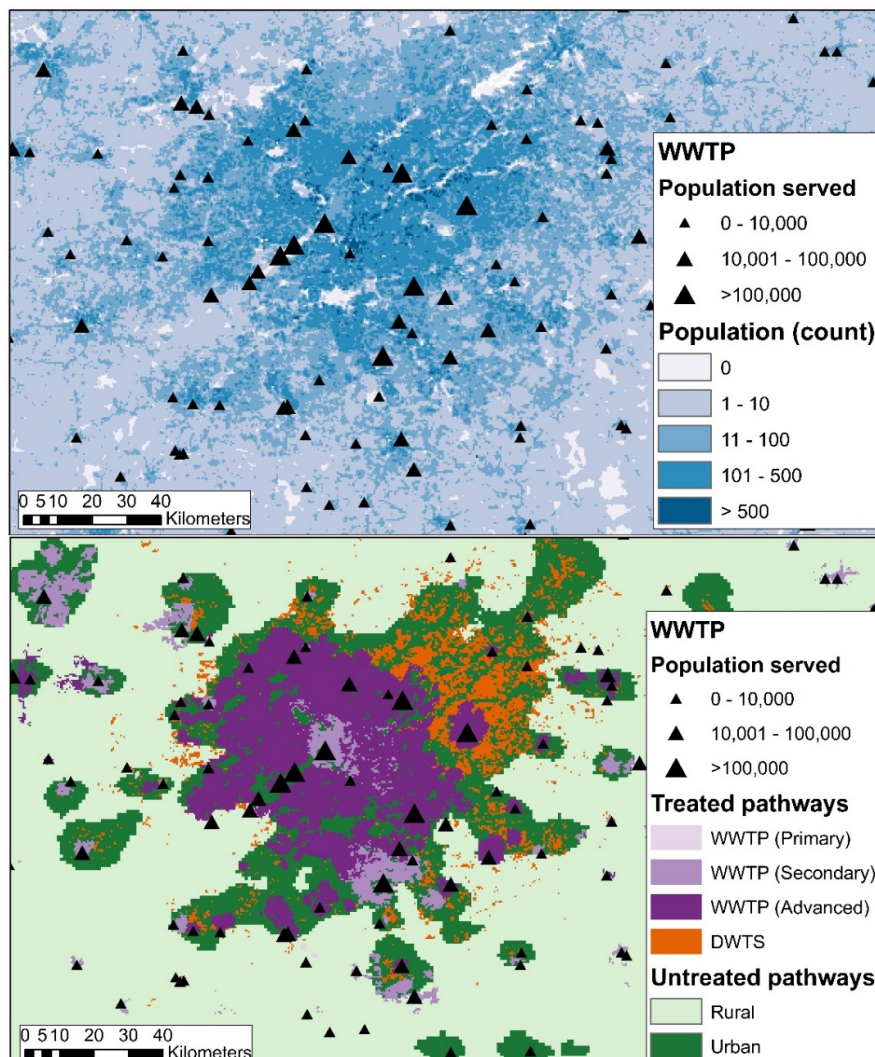
Figure 2. Example of the location of WWTPs and the population distribution (top panel) and the modeled contaminant pathway allocation (bottom panel) for the Atlanta metropolitan area in the United States. The areas shaded in purple (bottom panel) show the estimated service areas associated with individual WWTPs (black triangles). The populations residing in these areas are connected to the river network as point sources based on the discharge locations of their respective WWTPs. The populations residing in the orange areas (bottom panel) are identified as being associated with decentralized wastewater systems and are connected to the river network as diffuse but treated sources within the catchment of each river reach. The populations residing in the areas represented by shades of green (bottom panel) are associated with untreated wastewater contributions and are connected to the river network as diffuse sources within the catchment of each river reach.

First, populations are allocated to individual WWTPs. Although HydroWASTE provides details on the number of people served by a WWTP, it does not specify the spatial distribution of the population served nor the service area associated with it; that is, it does not provide explicit information that is required to spatially allocate the populations that are served versus those not served by WWTPs (top panel of Figure 2). The service area of a WWTP depends on several local factors not easily

220 obtainable at the global scale, such as decisions of the administrative unit responsible for the facility, and the distribution of underground pipes that transfer the wastewater to the facility. Studies have presented different approaches to associate the area contributing to a WWTP. For instance, Keller et al. (2006) defined it as the nearest upstream contiguous urban area from the WWTP discharge point within 2 km, estimating the population served by the WWTP based on the number of people in this contributing area. However, the largest WWTP in their study served only 32,000 people (expressed as population equivalent),

225 whereas HydroWASTE contains almost 5,000 WWTPs that serve more than 100,000 people. Kapo et al. (2017) and Grill et al. (2018) associated the WWTP service area to an administrative unit, but these studies were developed in countries where the information on administrative units is widely available (i.e., USA and China, respectively), which is not typically the case at a global scale.

To allocate explicit spatial population distributions to individual WWTP locations in HydroFATE, we developed a method

230 that follows the approach of Shakya (2017). This approach assumes that a WWTP can serve populations both upstream and downstream as wastewater can be pumped and directed in complex underground sewage systems. It also assumes that the service area of a WWTP can exceed the nearest contiguous urban area, with larger WWTPs typically serving larger distances and populations. Shakya (2017) tested different buffer sizes (i.e., from 5 km to 30 km at 5 km increments) in India, to determine the best-fit service area for different WWTP sizes by comparing the population within the buffer to the reported number of

235 population served. Since distribution and characteristics of WWTPs in different regions of the world can vary substantially, we expanded upon this approach by using an iterative process instead of pre-defined buffer sizes.

The final WWTP allocation method assigns populations from the WorldPop population grid (WorldPop & CIESIN, 2018; see Section 2.3) to the point locations of WWTPs using a ranking system as described in detail in Section S.1 of the supplementary material. The method considers the distance of each population pixel from the WWTP, the size of the population served by

240 the WWTP, whether a population pixel is categorized as 'urban' or not, and whether candidate pixels are clustered in contiguous areas. The settings and thresholds applied in this method were initially set to those reported by Shakya (2017) and were then refined and finalized in a successive trial-and-error approach in which intermediate results were mapped, visually inspected for plausibility, and statistically tested to verify whether they led to further improvements. The final allocation procedure assigns population pixels to individual WWTPs until the reported total of served population of each WWTP was

245 reached, or until maximum distance thresholds are exceeded. Once the allocation is completed, the contaminant pathway from each allocated population pixel to the river reach is defined by the WWTP discharge location and can be separated into one of three treatment levels (primary, secondary, or tertiary/advanced) as specified in HydroWASTE (purple colors in bottom panel of Figure 2).

Besides explicit WWTP pathways, HydroFATE also accounts for sources of potential contamination from decentralized
250 wastewater treatment systems (DWTS) that are not included in HydroWASTE, such as household septic tanks. To this end,
for every country, the difference was calculated between the aggregated population served by WWTPs according to
HydroWASTE and according to the global database on sanitation JMP-WASH (WHO & UNICEF, 2021). If JMP-WASH
reported higher numbers of population served, this difference was assigned successively to the pixels with highest population
numbers within the respective country borders that have not been allocated to WWTPs. The wastewater pathway type of these
255 pixels thus defaults to that of DWTS (orange color in bottom panel of Figure 2) and include a specific removal efficiency. In
the absence of explicit information, it is assumed that after DWTS treatment the effluent discharge directly enters the surface
drainage system at the pixel's location within a catchment and then flows to the catchment's associated river reach.

Finally, all remaining population pixels that were not assigned in any of the previous steps were considered to be diffuse
wastewater sources and were classified as 'untreated' (green colors in bottom panel of Figure 2). They were separated between
260 rural and urban using an urban area grid (see Section 2.3). All population pixels classified as diffuse sources thus have a defined
contaminant pathway that goes from the pixel's location within a catchment to the catchment's associated river reach. The
contaminant removal along this pathway in soils and the subsurface is determined through distinct urban vs. rural attenuation
functions.

3.2 Incorporation of contaminant pathways into HydroFATE

265 The results of the various population allocation steps described above are used as inputs into the HydroFATE model. The total
input of contaminants from treated pathways into each river reach is the sum of the contributions from all WWTPs (i.e., point
sources) releasing wastewater into that reach and the contribution from populations served by DWTS (i.e., decentralized
sources):

$$L_{t,r} = \left(\sum_i^r \left(P_{WWTP,i} \times \left(1 - \frac{e_{WWTP,j}}{100\%}\right)\right) + \left(\sum_m^c P_{DWTS,m} \times \left(1 - \frac{e_{DWTS}}{100\%}\right)\right)\right) \times L_{cap} \qquad (1)$$

270 where $L_{t,r}$ is the total load of the contaminant in river reach r originating from treated pathways in the reach catchment c
contributing to r (g day^{-1}); $P_{WWTP,i}$ is the population (persons) served by each WWTP i connected to river reach r; $P_{DWTS,m}$ is
the population (persons) served by DWTS from pixel m inside catchment c; L_{cap} is the per capita load (excreted) of the
contaminant (g cap^{-1} day^{-1}); and $e_{WWTP,j}$ and e_{DWTS} are the removal efficiencies (%) of WWTPs and DWTS, respectively,
releasing wastewater into the reach at treatment level j (primary, secondary, or advanced).

275 To estimate the diffuse contributions from populations in urban and rural areas who are not served by wastewater treatment
systems, it is assumed that not all human releases of untreated wastewater enter directly into surface waterbodies. This is due
to various processes of natural attenuation such as absorption in soils or deposition in land surface depressions (Lapworth et
al., 2012). Unfortunately, the factors affecting the natural attenuation and partial release of effluents are currently not well
understood. Therefore, a proxy variable termed the direct discharge coefficient is incorporated into the model to represent the

fraction (dimensionless) of contaminant load from untreated pathways that reaches a waterbody after processes of natural
attenuation. For example, for baseline model applications (see Section 4), the direct discharge coefficient for urban populations
was set to 0.8 and for rural populations to 0.5, respectively, following Grill et al. (2018). The higher coefficient value for urban
areas is due to the presence of impervious surfaces leading to more direct disposal of wastewater to nearby rivers and streams.
The total input of contaminants from untreated pathways to each river reach is then calculated as:

$$L_{u,r} = \left(\left(\sum_m^c P_{urb,m} \times ddc_{urb} \right) + \left(\sum_m^c P_{rur,m} \times ddc_{rur} \times F_m \right) \right) \times L_{cap} \tag{2}$$

where $L_{u,r}$ is the total load of the contaminant arriving at reach r from all untreated pixels m inside the reach catchment c (g
day^{-1}); L_{cap} is the per capita load (excreted) of the contaminant (g cap^{-1} day^{-1}); $P_{urb,m}$ and $P_{rur,m}$ are the total count of
population (persons) following the untreated pathway from pixel m, in urban and rural areas, respectively; and ddc_{urb} and
ddc_{rur} (dimensionless) are the direct discharge coefficients representing the proportion of contaminant load from untreated
pathways that are discharged into the river reach r from urban and rural areas respectively. F_m (dimensionless) is a factor by
which loads from rural populations are additionally reduced based on an inverse distance relationship that accounts for limited
connectivity in areas that are further away from the river network, following the approach by Grill et al. (2018):

$$F_m = \left(D_{m,r} + 1 \right)^{-1} \tag{3}$$

where F_m (dimensionless) represents the fractional distance-based contribution factor for pixel m; and $D_{m,r}$ (kilometers) is the
Euclidean distance between the pixel m and the river reach r. This equation delivers fractional contribution values between 0
and 1, with 1 for locations closest to the river, 0.5 at a distance of 1 km, and continuously decreasing values as the distance
increases. In contrast to the original method used in Grill et al. (2018), we refrained from normalizing the factor (i.e., by
constraining F_m to 0 at the furthest distance in each reach catchment), considering that contaminant contributions from any
distance can reach the river system. Also, we used Euclidean distances rather than distances along the surface hydrological
flow path (as proposed by Grill et al. 2018) assuming that contaminants can also travel through soils and groundwater. We
tested the sensitivity of the parameter settings by doubling and halving both the distance value and the exponent in Equation
3, finding that the resulting uncertainty ranges were below those of other model parameter settings.

3.3 River and lake routing

The mass transport in HydroFATE follows a 'plug-flow' approach (Pistocchi et al., 2010). That is, a 'plug' of substance mass
is accumulated downstream as the sum of the input from the current and all upstream reaches flowing into the current reach
(Grill et al., 2018):

$$L_{a,r} = \left(L_{t,r} + L_{u,r} + \sum_n L_n \right) \times d_{s,r} \times d_{l,r} \tag{4}$$

where $L_{a,r}$ represents the total load of the contaminant accumulated at the end of river reach r (g day⁻¹), calculated as the mass influx from treated pathways ($L_{t,r}$) plus the mass influx from untreated pathways ($L_{u,r}$) plus the total load (after decay) from those upstream reaches n ($\sum_n L_n$) that directly discharge into reach r, multiplied by the instream decay factor $d_{s,r}$ (dimensionless) and the lake decay factor $d_{l,r}$ (dimensionless) that apply at reach r. The instream degradation of a chemical substance in the river body, if applicable, is expected to decrease at a rate proportional to its mass, and is calculated assuming first-order decay:

$$d_{s,r} = e^{-kt_r} \tag{5}$$

where $d_{s,r}$ (dimensionless) is the instream decay factor for reach r, t_r is the time a plug of water needs to travel through the river reach r (days), and k is a first-order decay constant specific to the contaminant (day⁻¹), which determines the rate of environmental decay in the river (Grill et al., 2018). Note that the inverse of k represents the half-life of the chemical in the environment.

As an important partial contaminant sink, lakes were integrated and modelled as 'completely stirred reactors' (CSTR) (Anderson et al., 2004). The degradation of a chemical substance in lakes within the river network is calculated:

$$d_{l,r} = \frac{Q_r}{Q_r + (k \times V_r)} \tag{6}$$

where $d_{s,r}$ (dimensionless) is the instream decay factor for reach r, Q_r is the river discharge (L day⁻¹) at the river reach r; k is the first-order decay constant specific to the contaminant (day⁻¹); and V_r is the combined volume (L) of all lakes along river reach r. The locations and characteristics of lakes in HydroFATE are derived from the global lake database HydroLAKES (Messager et al., 2016). If there are no lakes in the river reach, $d_{l,r}$ is equal to 1.

To calculate the Predicted Environmental Concentration (PEC_r) of the contaminant at river reach r (ng L⁻¹), the final contaminant load (after any accumulation or removal) at reach r ($L_{a,r}$; g day-1) is divided by the river discharge (Q_r; L day⁻¹) at the same location:

$$PEC_r = \frac{L_{a,r}}{Q_r} \times \frac{10^9 \text{ ng}}{1 \text{ g}} \tag{7}$$

4 Model application and performance evaluation: concentration of sulfamethoxazole in the global river network

To evaluate the global applicability and general performance of the HydroFATE model, including the new distinction into six contaminant pathways as described in Section **Error! Reference source not found.**, the model was used in a proof-of-concept study to predict the distribution of the antibiotic sulfamethoxazole (SMX) in the global river network. SMX is considered a contaminant of emerging concern (Wilkinson et al., 2022), and selected due to a relatively high level of data availability, including global per capita consumption and metabolism fraction, WWTP removal efficiency and instream decay constants, and Measured Environmental Concentrations (MECs) reported for numerous rivers and streams around the world. The PECs

in surface waters were calculated based on long-term naturalized discharge as provided for all river reaches in the RiverATLAS database (Linke et al., 2019). The resulting PECs were compared to MECs to evaluate the model's predictive ability. Furthermore, PECs were also used to assess the exposure associated with SMX based on a comparison of PECs in surface

340 waters relative to the reported Predicted No-Effect Concentration (PNEC), which is the concentration threshold below which no adverse effects of exposure are observed in laboratory-based toxicity tests (Archundia et al., 2018; Hernando et al., 2006). Finally, to further assess the model's performance under a range of alternative conditions, HydroFATE was run for a total of four scenarios based on plausible ranges of configuration settings and parameters extracted from literature sources.

4.1 Input data

345 **4.1.1 SMX properties**

Sulfamethoxazole (SMX) is a sulfonamide antibiotic, usually sold in combination with trimethoprim. When consumed, SMX is rapidly absorbed upon oral administration, with metabolism mainly hepatic (Rudy & Senkowski, 1973). Residues are mostly excreted in urine, and the proportion of unchanged substance can be between 10 and 30%, depending on urine pH (Straub, 2016). Based on a comprehensive literature search, Straub (2016) found 36 publications that reported 190 removal efficiencies

350 of SMX in WWTPs, with an average of 21% removal, a median of 49%, and an interquartile range from 2% to 73%. Archundia et al. (2018) compiled 6 different studies that measured environmental decay in rivers, finding an average first-order decay constant of 0.73 day^{-1}, a median of 0.13 day^{-1}, a minimum of 0.034 day^{-1}, and a maximum of 2.88 day^{-1}.
For the main mode run in this study, the average excretion fraction and the median values of wastewater removal efficiency and instream decay constant were used (see Table 1, baseline scenario). But we also explored the ranges of possible values

355 and how they affect the model outputs (see Table 1, alternative scenarios; for more details see Section 4.2.1. below). Since Straub (2016) does not provide specific removal efficiencies for SMX for different treatment levels of WWTPs, the same removal efficiency was assumed for primary, secondary, and advanced treatment levels.

4.1.2 SMX global consumption

Country-level averages of annual consumption per capita of SMX were necessary to estimate emissions to the river network.
360 Klein et al. (2018) analyzed and estimated the consumption of various antibiotics in the world based on the IQVIA database, which reports annual sales for the period of 2012 to 2015 for 91 countries. For our study, the annual consumption of SMX for each country was assumed to be the average between the four available years as provided by Klein et al. (2018). For countries not included in the IQVIA database, the consumption rate was extrapolated based on the average per capita SMX use from the same income group (World Bank, 2019) following the methodology described by Klein et al. (2018).

4.1.3 Measured Environmental Concentrations (MECs)

To evaluate the predictive ability of HydroFATE, 227 data points of MECs were compiled from literature sources (see Figure 3 for their location and see Section S.2 in the supplementary material for literature sources). MECs are reported from every continent except Oceania. The average of reported values is 390 ng L^{-1}, the median is 28 ng L^{-1}, the minimum is 0.23 ng L^{-1}, and the maximum is 21,000 ng L^{-1}. In addition, 134 non-detects (i.e., concentrations reported were lower than could be detected based on the analytical method used to measure SMX in water samples) were compiled. In order to be selected for inclusion as a MEC in our model evaluation, the literature source had to: (1) report the specific location (i.e., in the form of coordinates, river names, or river intersections) of the measurements; and (2) confirm that in the catchment feeding the river the dominant use of antibiotics is not through veterinary or industrial activities since the current version of HydroFATE is not adapted to account for these sources. Most MECs reported do not include corresponding comprehensive information on the river characteristics, such as width or average discharge which would have helped to identify the precise location in the river network, or on the conditions under which the measurement was taken, such as actual discharge amount or flow season (i.e., low flow, average, or high flow). Therefore, the actual location and amount of the reported MEC may not always accurately correspond to the referenced river network location and/or the assumed flow conditions in HydroFATE.

4.1.4 Predicted No-Effect Concentration (PNEC)

Since reports of SMX detection in rivers and streams first began to appear, its potential impact on the environment and human health has been assessed in several ways. That is, for exposure assessments, PNEC values often serve as thresholds to evaluate the level of environmental exposure to contaminants (Hernando et al., 2006). There are two values of PNEC for SMX published to-date in literature. First, the PNEC-Minimum Inhibitory Concentration (PNEC-MIC), for which a value of 16,000 ng L^{-1} was estimated by Bengtsson-Palme and Larsson (2016), is intended to be protective of antibiotic resistance. Second, the PNEC-Environment (PNEC-ENV), for which a value of 600 ng L^{-1} was estimated by Ferrari et al. (2004), is based on eco-toxicology data and is intended to protect aquatic function. For the purposes of the present case study, the lower value of PNEC (600 ng L^{-1}) was selected to protect against any possible impact in the exposure analysis.

4.2 Model application

4.2.1 Scenarios

A total of four main scenarios were created to portray plausible settings of parameters and model configuration, as outlined in Table 1. Scenario 1 represents baseline conditions using input parameters and model configurations that are expected to yield the most plausible predictions for average-flow conditions based on reported values in literature as described in Section 4.1.1. Scenario 2 represents low-flow conditions, but otherwise maintains the same parameters and configuration settings as Scenario 1. Scenarios 3 and 4 represent low-end and high-end settings, yet still within plausible ranges. That is, Scenario 3 (conservative case) uses parameter and configuration settings that represent minimum load emissions and maximum removal efficiencies

(including full substance removal in lakes) to represent low-end contaminant concentrations in the river network, and vice versa for Scenario 4. Additional scenarios (see Table S-3 in the supplementary material) were designed for the model performance evaluation to analyze the individual contributions of selected parameters and model configurations on the output, including a worst-case scenario assuming that no removal processes affect the contaminant load.

400 **Table 1. Scenarios designed to represent plausible parameter and model configuration settings to simulate the global distribution of SMX in rivers. Excretion fraction is the fraction of the consumed amount of SMX that is excreted after metabolism. Wastewater treatment removal efficiency is the percentage of SMX that is removed in treatment facilities (WWTPs or DWTS). For other parameters and configurations see text.**

	Scenario	Parameter settings					Configuration settings	
		Excretion fraction	Wastewater treatment removal efficiency (%)	Direct discharge coefficient		Instream decay constant k (day^{-1})	Lake removal	Discharge condition
				Urban ddc_{urb}	Rural ddc_{rur}			
1	*Baseline, average-flow*	0.2	49	0.8	0.5	0.13	CSTR removal	Average-flow
2	*Baseline, low-flow*	0.2	49	0.8	0.5	0.13	CSTR removal	Low-flow
3	*Low-end case*	0.1	73	0.2	0.2	2.88	Full removal	Average-flow
4	*High-end case*	0.3	2	0.9	0.9	0.03	No removal	Low-flow

4.2.2 Exposure assessment

405 The ratio of PEC to PNEC was used as an indicator to designate levels of SMX in the global river network that can lead to environmental health concerns. For that purpose, risk quotients, $RQ_{r,S}$ (dimensionless), were calculated for every river reach r and every scenario configuration S using the value of PNEC for SMX of 600 ng L^{-1} and the calculated $PEC_{r,S}$ (ng L^{-1}) at every reach r for the respective scenario S:

$$RQ_{r,S} = \frac{PEC_{r,S}}{PNEC} \tag{8}$$

410 In instances where the risk quotient is greater than or equal to 1 ($RQ_{r,S} \geq 1$), it is assumed that this exposure level can cause negative environmental impacts (Archundia et al., 2018; Hernando et al., 2006).

4.2.3 Performance evaluation

The performance of the model was evaluated by comparing reported MECs of SMX (see Section 4.1.3) and PECs calculated using HydroFATE at the coinciding river reaches. The goodness-of-fit indicators used to quantify model performance included

415 the normalized root mean square error (NRMSE), the percentage of bias (PBIAS), the Nash-Sutcliff efficiency coefficient (NSE; Nash & Sutcliffe, 1970), and the Kling-Gupta efficiency coefficient (KGE; Gupta et al., 2009). Besides the baseline calculations of Scenario 1, Scenarios 3 and 4 were evaluated as they benchmark plausible low-end and high-end variations of parameter and configuration settings, and Scenarios 5-7 (including 14 sub-scenarios, see Section S.3 in supplementary information) were developed to specifically test the uncertainty ranges introduced by individual parameter and configuration

420 settings.

4.3 Case study results

4.3.1 Global emission of SMX to rivers

The global consumption of SMX from the world's population is estimated at 2.6 million kg y^{-1}. From these, 2.4 million kg y^{-1} are consumed by populations with emission pathways that can potentially reach the river and lake system (including processes of metabolism, excretion, treatment, and/or natural attenuation), while the remaining 0.2 million kg y^{-1} are consumed by populations with direct emission pathways to the ocean. For the baseline scenario (Table 1), a total of 214,000 kg y^{-1} of SMX (9% of global consumption) are estimated to reach rivers and lakes (Table 2). From this, 29% are from pathways with some form of wastewater treatment (WWTP or DWTS) versus 71% from untreated pathways. The results show that although most of the consumption occurs among rural populations without access to treatment (i.e., 52% of total consumption), natural attenuation, as simulated in this study, has a high potential to remove the substance in rural areas before it reaches the rivers (i.e., resulting in only 30% of total emission to rivers and lakes). In contrast, populations in urban areas without access to wastewater facilities were modelled to have the highest emissions to the river and lake network (i.e., 42% of total emissions). The processes simulated in this study that are responsible for removing portions of the substance along its way from the consumer to the final destination at the ocean or an inland sink are, in order of quantity removed: metabolism (80% of total consumption is removed), natural attenuation in rural areas (7.5%), instream decay (3.5%), wastewater treatment in WWTPs and DWTS (2.4%), lake removal (1.7%), and natural attenuation in urban areas (1.0%). The total SMX reaching the ocean or an inland sink through rivers amounts to 92,200 kg y^{-1} (3.9% of global consumption).

Table 2 shows the 20 countries that are estimated to have the largest emissions of SMX. India accounts for the highest national emission to rivers and lakes (30,500 kg y^{-1}), despite its lower-than-average per capita consumption (801 µg day^{-1}). This is due to a combination of large populations and a lack of access to wastewater treatment in urban areas. South Africa shows the highest per capita consumption (6,220 µg day^{-1}), while China shows one of the lowest (67 µg day^{-1}), but it is still among the top 20 emitters.

455

Table 2. Top 20 countries ranked by their predicted emissions of SMX to rivers and lakes, their population sources, and their emission and consumption rates by pathway, and global totals. For a complete list of all countries see Table S-4 in the supplementary material.

Country	Population source (%)			Consumption		Total emission to rivers and lakes	Emission to Consumption ratio	Contaminant pathway into rivers or lakes (%)		
	Treated (WWTPs and DWTS)	Urban untreated	Rural untreated	Total (kg y⁻¹)	per capita (µg day⁻¹)	(kg y⁻¹)	(%)	Treated (WWTPs and DWTS)	Urban untreated	Rural untreated
India	6.1	24.8	69.1	366,000	801	30,500	8.3	7.4	47.8	44.8
United States	76.6	10.0	13.4	291,000	3,070	28,200	9.7	76.3	16.5	7.2
Pakistan	6.8	29.7	63.5	224,000	3,150	19,500	8.7	7.9	54.5	37.6
South Africa	28.8	41.6	29.6	102,000	6,220	11,200	11.0	26.7	60.4	13.0
Brazil	29.2	41.4	29.4	77,400	1,190	8,670	11.2	26.0	59.1	14.9
Mexico	41.0	38.3	20.7	62,400	1,500	7,310	11.7	37.1	52.8	10.1
Indonesia	4.4	32.2	63.4	74,800	904	7,170	9.6	4.6	53.8	41.6
Nigeria	2.0	22.3	75.6	82,200	1,240	6,430	7.8	2.7	45.7	51.7
Egypt	41.1	34.5	24.5	55,500	1,920	6,020	10.8	38.2	50.8	11.0
Iran	22.8	37.1	40.1	34,700	1,260	3,630	10.5	22.2	56.8	21.0
Bangladesh	4.8	24.5	70.6	39,400	714	3,440	8.7	5.7	45.2	49.2
Russia	49.3	22.0	28.7	33,000	696	3,190	9.7	46.9	36.4	16.7
Vietnam	1.0	27.7	71.3	33,400	1,030	2,890	8.7	1.2	51.2	47.6
China	43.5	9.6	46.9	31,900	67	2,760	8.7	51.0	18.2	30.8
DR Congo	0.3	18.0	81.7	39,700	1,240	2,750	6.9	0.4	41.8	57.8
Ethiopia	1.2	9.9	88.9	40,400	1,210	2,450	6.1	2.0	26.1	71.9
Ecuador	28.3	35.3	36.4	22,700	4,130	2,430	10.7	27.0	52.9	20.2
Germany	94.9	0.2	4.9	22,700	816	2,260	10.0	97.3	0.3	2.4
Colombia	42.4	26.8	30.9	20,900	1,090	2,190	10.5	41.2	41.4	17.4
Algeria	31.0	30.8	38.3	19,500	1,730	1,960	10.1	31.4	48.9	19.7
Total	**26.1**	**20.9**	**53.0**	**1,670,000**	**1,700**	**155,000**	**9.3**	**28.7**	**43.3**	**28.0**
Global	**27.3**	**20.6**	**52.1**	**2,370,000**	**1,074**	**214,000**	**9.0**	**27.8**	**41.9**	**30.3**

Overall, the spatial patterns of contaminant emissions to rivers and lakes are very similar to the global patterns of consumption, with an average emission to consumption ratio of 9.0% (Table 2). In Ethiopia, the ratio of emission to consumption was predicted to be on the low end (6.1%), which is mostly due to the population being predominantly rural without access to treatment (89%) contributing to 72% of the total emission of SMX. In contrast, other countries such as Mexico, Brazil, and South Africa have a ratio above the global average (12%, 11%, and 11%, respectively) due to the main source of SMX being untreated urban pathways (i.e., impervious surfaces with less attenuation) or treated pathways (i.e., wastewater treatment removal efficiency for SMX is lower than the assumed proportion of SMX removed by processes of natural attenuation in rural areas).

Figure 3 illustrates the resulting spatial distribution of SMX concentrations in the global river network for the two baseline scenarios: Scenario 1 corresponding to average-flow conditions and Scenario 2 corresponding to low-flow conditions. Generally, higher concentrations are predicted for rivers in countries with high emissions, such as India, United States, Pakistan, and South Africa. Nonetheless, even in countries that are not among the highest emitters, such as many African countries, low river discharges can cause high concentrations of contaminants in the rivers, especially during low-flow conditions.
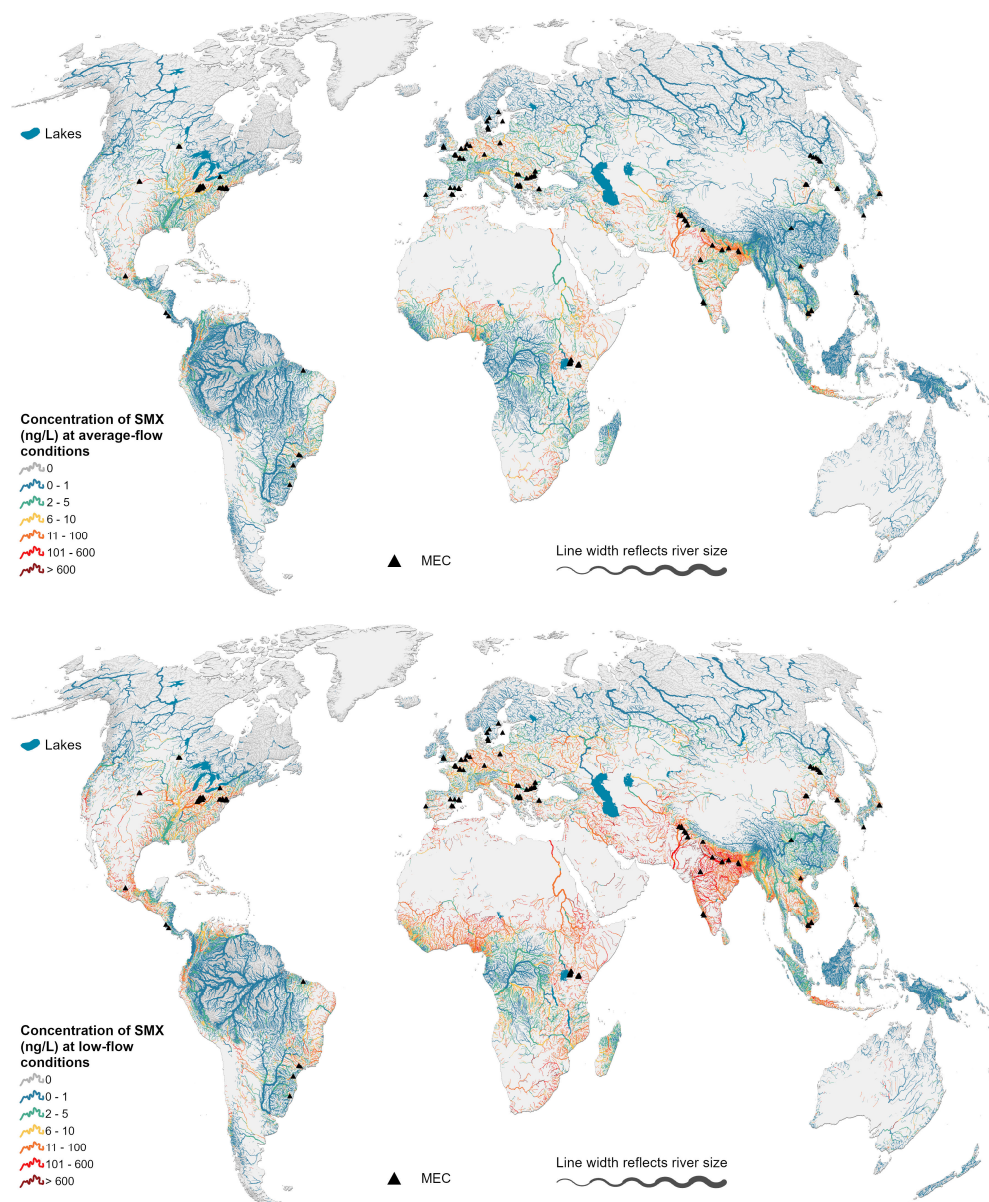
Figure 3. Estimated concentrations of sulfamethoxazole (SMX) in the global river network using the HydroFATE model for baseline Scenarios 1 (top panel, average-flow conditions) and 2 (bottom panel, low-flow conditions). See Table 1 for scenario settings. The black triangles represent the locations of Measured Environmental Concentrations (MECs) used in the model evaluation. For visual clarity, only rivers exceeding a long-term average flow of 3 m³ s⁻¹ are shown on the map.

4.3.2 Exposure assessment

480   The results of baseline Scenario 2 (low-flow conditions) predict aquatic exposure to SMX concentrations above the PNEC (i.e., risk quotient ≥ 1) for 1.6% (i.e., 390,000 km) of all rivers in the world with long-term annual average discharge above 0.1 m³ s⁻¹ (Table 3). India, Pakistan, and Sudan show the largest extent of rivers in this category which indicates a potential risk for environmental health. This percentage decreases to 0.1% (corresponding to 30,100 km) for baseline Scenario 1, i.e., when average-flow conditions are assumed. Pakistan has a particularly high percentage of rivers in the risk category for both

485   scenarios (i.e., 33.5% and 8.4% of all rivers for Scenarios 2 and 1, respectively).

Table 3. Top 20 countries by total length of rivers with a predicted risk quotient (RQ) ≥ 1 for SMX for Scenarios 2 (low-flow conditions) and 1 (average-flow conditions).See Table 1 for scenario settings. The total length of rivers is extracted for each country from the RiverATLAS database (Linke et al., 2019) accounting for all rivers in the world with long-term annual average discharge above 0.1 m³ s⁻¹ (i.e., a global total of 23.9 million km). The increase in length of rivers presenting risk of exposure based on specific
490   **conditions was calculated by running the model for the pertinent scenario but changing the parameters and configurations accordingly. See Table S-5 in the supplementary material for a complete list of all countries.**

Country	Total length of analyzed rivers (km)	RQ ≥ 1 at low-flow conditions				RQ ≥ 1 at average-flow conditions			
		Length of rivers (km)	% of total length	% increase in length without instream decay	% increase in length without lake removal	Length of rivers (km)	% of total length	% increase in length without instream decay	% increase in length without lake removal
India	776,000	111,000	14.3	8.2	16.9	3,630	0.5	12.3	30.7
Pakistan	102,000	34,200	33.5	7.4	3.9	8,600	8.4	5.6	3.9
Iran	201,000	16,800	8.3	6.8	2.5	1,120	0.6	2.2	3.3
Sudan	100,000	15,200	15.1	7.7	1.5	344	0.3	24.8	26.8
South Africa	107,000	12,500	11.6	13.8	51.0	3,540	3.3	30.6	73.6
United States	1,780,000	11,800	0.7	14.6	29.3	1,330	0.1	22.5	65.2
Saudi Arabia	72,300	11,600	16.0	12.7	0.1	84.2	0.1	14.4	6.0
Ethiopia	185,000	10,800	5.8	14.0	2.8	301	0.2	5.7	24.2
Mexico	270,000	10,400	3.8	9.3	26.8	1,370	0.5	10.4	22.6
Algeria	94,100	8,990	9.6	6.9	10.6	985	1.0	16.1	16.4
Nigeria	201,000	8,880	4.4	8.0	13.1	525	0.3	46.8	91.4
Yemen	22,200	8,170	36.8	3.1	0.1	771	3.5	4.6	2.0
Niger	49,900	7,960	15.9	8.2	7.8	292	0.6	41.0	59.5
Somalia	42,500	7,280	17.2	6.8	0.0	17.3	0.0	96.0	0.0
Iraq	36,600	5,960	16.3	5.0	7.5	211	0.6	19.3	9.4
Chad	85,100	5,910	6.9	11.1	3.0	64.5	0.1	15.0	70.9
China	1,440,000	5,730	0.4	17.1	21.9	43	0.0	60.9	124.3
Afghanistan	79,500	4,570	5.8	12.0	0.2	108	0.1	11.9	0.0
Oman	13,900	4,540	32.6	4.6	0.5	0	0.0	0.0	0.0
Brazil	2,410,000	4,160	0.2	5.2	20.7	411	0.0	1.3	4.1
Total	**8,070,000**	**306,000**	**3.8**	**8.8**	**12.8**	**23,700**	**0.3**	**13.7**	**27.0**
Global	**23,900,000**	**390,000**	**1.6**	**9.1**	**14.6**	**30,100**	**0.1**	**13.7**	**25.3**

     To assess the contribution of instream decay processes (i.e., decay in rivers and removal in lakes) to the reduction in contaminant concentrations, the increase in length of rivers with SMX concentrations exceeding PNEC was calculated

495   assuming that these processes are not taking effect (i.e., the respective first-order decay constant *k* is set to 0). Globally, if both river and lake environmental decay processes were omitted, there would be a combined increase of 23.7% and 39.1% in the length of rivers that fall in the risk category compared to Scenarios 2 and 1, respectively (Table 3). If only lake removal processes were excluded, there would be an increase of 14.6% in Scenario 2 and 25.3% in Scenario 1. Lake removal is predicted

to be particularly important in rivers in South Africa, United States, Mexico, and China. For instance, without lake removal,
500   there would be an increase of 51% of rivers in South Africa falling in the risk category at low-flow conditions.

Finally, to demonstrate the utility of a contaminant fate model operating at high spatial resolution, Figure 4 depicts the risk
distribution under low-flow conditions (Scenario 2) for the region of Southeast Asia, including the two countries (India and
Pakistan) with the longest total length of rivers in which SMX concentrations exceed PNEC. The high spatial resolution permits
the detection of local increases in risk immediately downstream of individual WWTPs, which then can diminish along the
505   flow paths once inflowing tributaries cause dilution effects. Model results also reveal the exposure of individual rivers
receiving contaminant discharge without any treatment (i.e., areas without any black dots but presenting a high density of
rivers at risk).
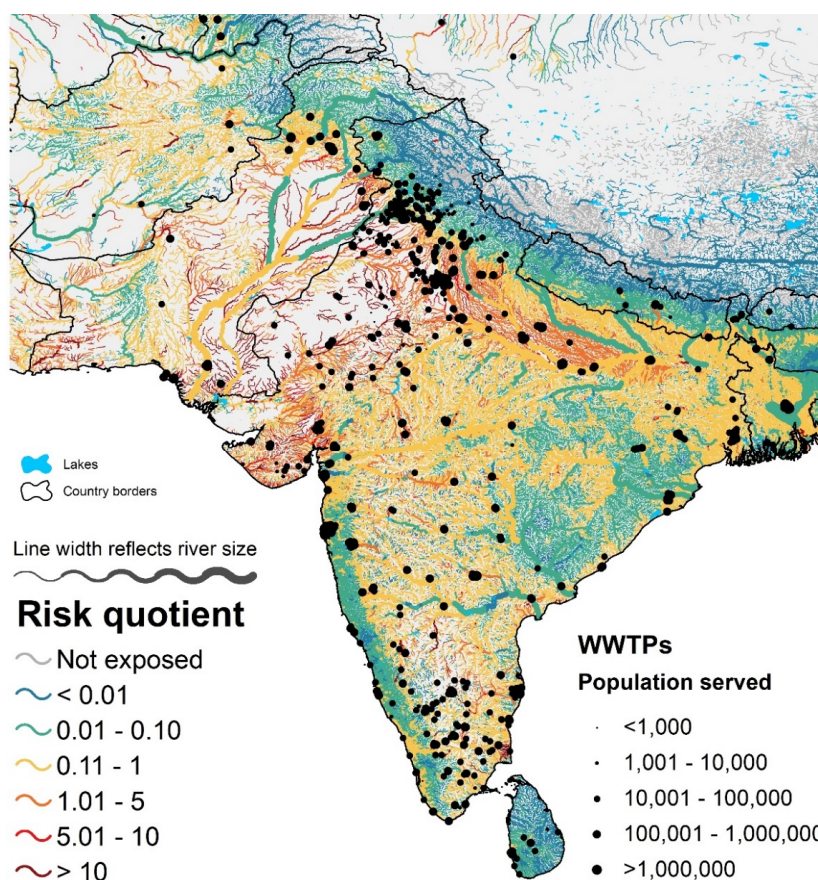
Figure 4. Estimated risk quotient for sulfamethoxazole (SMX) using HydroFATE in parts of Southeast Asia, with a focus on India
510   **and Pakistan. The risk quotient was calculated using Scenario 2 (see Table 1 for scenario settings). The black dots represent the**
location of wastewater treatment plants (WWTPs) in the database HydroWASTE. For visual clarity, only rivers exceeding a long-
term average flow of 0.1 m^3 s^{-1} are shown on the map.

4.4 Performance evaluation

Modelling results were evaluated by comparing predicted SMX concentrations with available measurements in river reaches
515   across the world using 227 MECs with values above the detection threshold. Figures 5(a) to (d) show an analysis of results for
baseline Scenario 1 (average-flow conditions; see Table 1 for scenario settings), stratified by certain characteristics of the
measurements. The different colors of points in the overall scatter plot shown in Figure 5(a) illustrate the global distribution
of measurements. The African continent presents the highest SMX concentrations (both measured and predicted) and the
predicted concentrations in Asia, Europe and Central America are in their majority below reported measured concentrations.
520   These results confirm that model predictions for Scenario 1 are generally reasonable, with 79% of the predicted values being
within one order of magnitude of the measured concentrations reported in literature (Johnson et al., 2008, Oldenkamp et al.,
2018).

Figure 5(b) shows the different model performance indicators when comparing all 227 MECs against estimates derived for
Scenario 1, reflecting overall fair results yet with a clear bias towards modelled concentrations being lower than reported
525   measurements. Since there is a possibility that some of the MECs were measured during low-flow conditions (Section 4.1.3),
the comparison with results using Scenario 1 (representing average-flow conditions) might not be appropriate. To explore this
issue further, error bars were added into Figure 5(b), where the ends of the error bars (extending only leftwards) show a
recalculated MEC for average discharge conditions when assuming that the original concentration of SMX was measured
during low-flow conditions. This analysis demonstrates that cases in which predicted values were too low could, in part, be
530   explained by uncertainties within the measurements rather than errors in the model predictions.
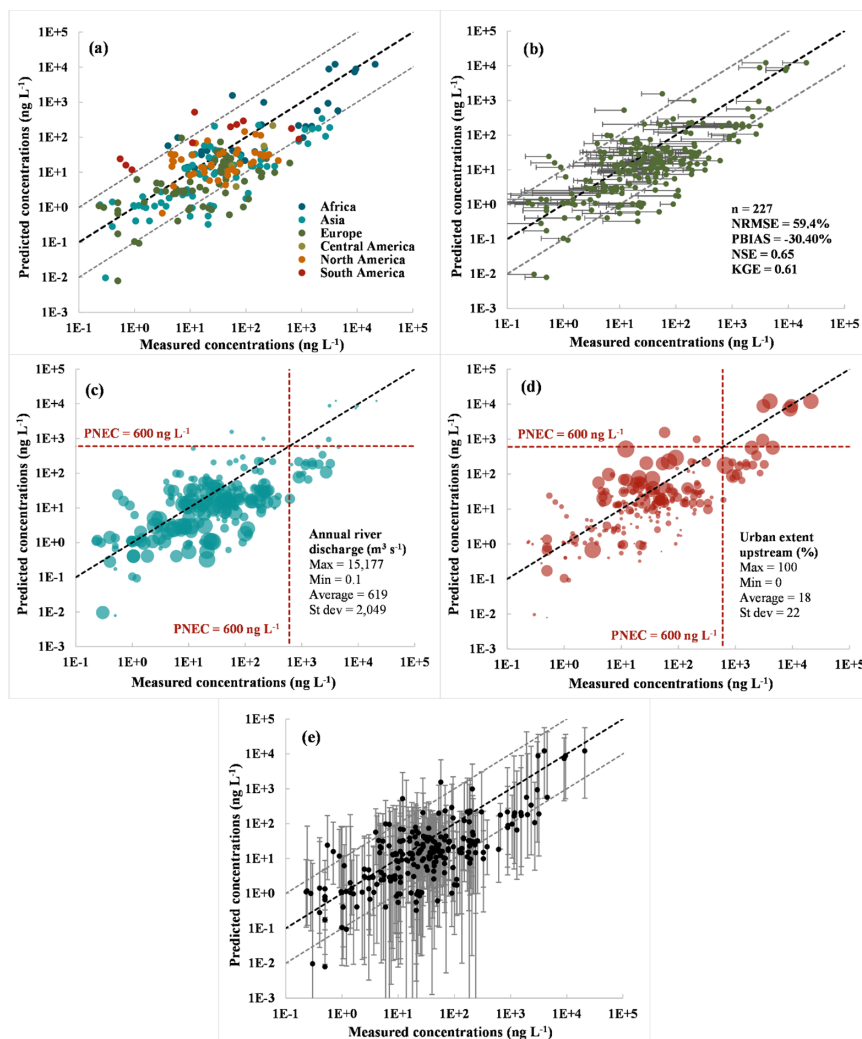
Figure 5. Evaluation of the SMX concentrations estimated using HydroFATE for baseline Scenario 1 (average-flow conditions; see Table 1 for scenario settings)ndividual points represent comparisons between Measured (MEC) and Predicted (PEC) Environmental Concentrations in the same river reach. The black dashed line represents the 1:1 line and the gray dashed lines represent the error line corresponding to one order of magnitude. Panel (a) shows a general scatter plot between MECs and PECs and indicates their spatial distribution (with different point colors representing the geographic regions). Panel (b) shows uncertainties of MECs regarding river discharge where the ends of the error bars represent a modified MEC assuming the original was measured during low-flow conditions; n is the number of records; NRMSE is the normalized root mean square error; PBIAS is the percent bias; NSE is the Nash-Sutcliffe efficiency; and KGE is the Kling-Gupta efficiency. Panel (c) indicates the annual river discharge at the river reach of the MEC in different bubble sizes; and panel (d) indicates the urban extent upstream of the river reach of the MEC in different bubble sizes; the red dashed lines represent the threshold for the PNEC. Panel (e) shows uncertainties of PECs where the error bars represent the range of resulting PECs using the parameter and configuration settings of Scenarios 3 and 4. Error bars that extend below 0.001 ng L⁻¹ may include predicted zero concentrations.

Figure 5(c) shows the same points with bubbles sized according to average discharge at the measurement location and Figure
5(d) shows bubbles sized according to upstream urban extents. Most measurement locations for which model predictions of
concentrations were too high are located downstream of urban populations on rivers with low discharge, which is a challenging
combination to model; that is, urban streams can be heavily modified by anthropogenic activities that influence their flow
quantities and water quality, such as channelization, dams, and sewers. Besides, if the urban population is not served by
WWTPs, the predictions were based on the assumption of a constant direct discharge coefficient, which in all probability is
variable in reality. Despite these uncertainties, only two measurements were predicted erroneously above the PNEC threshold,
resulting in a risk quotient that is falsely predicted to be above 1. On the other hand, 17 measurements were erroneously
predicted to be below the PNEC threshold, which is in accordance with the overall conservative approach and scenario
configuration used in this case study.

Finally, Figure 5(e) shows substantial uncertainties in PEC calculations (i.e., extent of error bars) when using the parameter
and configuration settings of Scenarios 3 and 4, representing low-end and high-end simulations that were within plausible
ranges. Taking these uncertainties into account, 78% of all MECs fell within the range of error bars of HydroFATE; i.e., they
were reproducible by the model within at least one of the chosen parameter and configuration setting.

In addition to the 227 MECs, 134 measurements were classified as 'not detected' or 'not quantified.' To evaluate these cases,
PECs at the same locations were verified to determine if they were correctly predicted to be below the detection or
quantification limit (LOD or LOQ, respectively), depending on the limit reported by the study. The rate of success was 60%,
and if allowing an error of one order of magnitude, the success rate increased to 93%.

In addition to the performance evaluation presented in Figure 5, three additional scenarios (including 14 sub-scenarios) were
analyzed to specifically test the uncertainty ranges introduced by individual parameter and configuration settings (see Section
S.3 in supplementary information for details). The results indicate that the model reacts sensitive yet within reasonable
boundaries to the permutations of individual parameter settings. Of particular importance are the settings related to substance
removal simulations in the model which depend on local characteristics and on the dominating pathway of the contaminant.

5 Discussion

5.1 HydroFATE: strengths and limitations

In this study, the first global application of the contaminant fate model (CFM) HydroFATE was presented, building upon
previous stages of the model that were used to assess the distribution of pharmaceuticals at the regional scale in Canada, China
and India. One of the main characteristics that distinguishes HydroFATE from other global CFMs, besides its high spatial
resolution, is that contaminant pathways are differentiated based on whether the wastewater undergoes treatment or not and,
if so, at what treatment level. Contaminants generated by populations connected to wastewater facilities are partially removed
by treatment processes, whereas contaminants generated by populations not connected to any wastewater system are assumed
to undergo natural attenuation processes, which in the case of rural populations also depend on how distant they are from any

waterbody. The model application showed that different regions indeed respond differently to pharmaceutical drug consumption depending on the main pathway of the contaminant before reaching the river system.

Despite its high spatial resolution, HydroFATE has primarily been designed as a CFM that operates at large scales, including at the global scale, and it can be readily applied with existing input data. Due to the necessary model simplifications to enable
580 such an approach, it is recognized that, even with anticipated future refinements, substantial uncertainties will remain with respect to the model's predictive capability. As such, HydroFATE is intended to serve as a screening model whose primary purpose is to identify critical areas where detailed field studies should be performed.

To apply any model appropriately and interpret its output, it is essential to understand its limitations. The main limitations of HydroFATE stem from its steady-state approach, the difficulty of capturing some underlying processes at the global scale, the
585 lack of information on the behavior, use and disposal of most CECs, and unaccounted variability regarding most input parameters of the model. HydroFATE transport processes are based on long-term average discharge or long-term monthly minimum discharge, which does not account for the seasonality of river flows or any shorter-term fluctuations that affect the dilution capabilities (or lack thereof) of contaminant concentrations. The decay of contaminants along rivers and in lakes is assumed to follow a first-order process, lumping and simplifying complex processes such as deposition, adsorption,
590 photodegradation, and bioaccumulation that occur over time. These processes also depend on local environmental and biological characteristics that are currently very difficult to capture at a global scale. Therefore, more experiments and measurements are needed to reduce the uncertainties inherent in quantifying the decay constants for different substances and under different conditions, especially contaminants of emerging concern. In the presented case study application, an average decay constant arising from only a few reports for sulfamethoxazole was used, which likely represents an overly narrow range
595 that does not adequately capture what happens under different conditions in rivers worldwide.

Wastewaters from almost half of the world's population are untreated. The uncertainties in HydroFATE related to contaminant simulations from untreated sources have two main sources: (1) the difficulty to spatially distinguish wastewater contributions from populations as treated or untreated in the first place, based only on WWTP characteristics, country-level statistics, and a global population grid; and (2) the generalization of the pathways of untreated contaminants into only two types (i.e.,
600 distinguishing only rural versus urban conditions) based on simplified assumptions and very little evidence from field experiments (Grill et al., 2018). In the presented case study, the untreated pathways contributed an estimated 72% of the global emission of sulfamethoxazole. Nonetheless, despite the large uncertainties, the baseline scenario was able to reproduce field measurements reasonably well, especially considering the large range of possible values for the critically important direct discharge coefficients (see Table 1). Panel (d) of Figure 5 suggests a general overestimation of contaminant concentrations in
605 regions with substantial urban extents upstream (larger bubbles) and a general underestimation for rural areas (i.e., smaller bubbles representing areas with smaller urban extents), an observation which could be used to revise the direct discharge coefficients in future model runs. However, to ensure that HydroFATE is generally applicable to a range of substances, it is recommended that the model be first tested when applied to other substances before a potential calibration of different direct discharge coefficients is carried out to improve model performance. In addition, as further discussed below, the current model

610   version only accounts for one type of source (domestic), which excludes veterinary and industrial contributions that can be present in waters, making any uncontrolled measurements inadequate for calibration.

Besides the river network, the pathways of the contaminants determine most of the spatial contaminant distribution of the model. The method developed in this study distinguishes the wastewater contributions from the global population as treated or untreated by relying mostly on global population and urban extent grids, and the global WWTP database HydroWASTE.

615   Both population and urban extent grids have their own uncertainties related to the way they have been developed, their spatial resolutions, and their representative years, potentially misrepresenting actual conditions especially in sprawling cities in developing countries (Sridhar & Mavrotas, 2021). HydroWASTE is a data compilation that contains estimated characteristics instead of official records for 9% of the WWTPs, and it does not include small DWTS that are more common in rural areas. In the absence of data, country-level statistics on sanitation were used to minimize these uncertainties regarding

620   HydroWASTE.

5.2 Performance evaluation of HydroFATE using sulfamethoxazole

As a first case study application of HydroFATE, country-level consumption data of sulfamethoxazole (SMX) were used to assess its distribution in the global river and lake network. Results predicted that a total of approximately 214,000 kg of SMX are released into rivers and lakes every year from domestic sources. A cursory exposure assessment shows that this release

625   may potentially result in a risk of environmental impact (i.e., defined as PEC ≥ PNEC) during low-flow conditions throughout 390,000 km of the global river network.

In terms of the input information regarding SMX, uncertainties can derive from various assumptions incorporated into the model parameters, including the country-level consumption rate, the excretion fraction (after metabolism), the wastewater treatment removal efficiency, and the instream decay constant. The contaminant emission is estimated based on country

630   averages of consumption and population density based on the assumption that every person consumes the same amount of SMX in a year across a country, which therefore does not account for regional, municipal, or personal (e.g., age-dependent) spatial variability of consumption. The excretion fraction has a relatively small range of uncertainty (Table 1) as the metabolism process of SMX inside the human body is well-known and was extensively studied by pharmaceutical companies before its release during the drug development phase (Zhang & Tang, 2018). The removal efficiency in treatment facilities, including

635   WWTPs and DWTS, depends on the specific type of treatment being employed. The values reported in the literature vary widely, possibly due to SMX being transformed to N4-acetyl-SMX and glucuronide conjugates (the most common SMX metabolites) and vice-versa during the treatment process (Straub, 2016). HydroFATE is, in principle, able to account for different levels of treatment provided by WWTPs (i.e., primary, secondary, or advanced) by using different removal efficiencies. However, due to a lack of consistent data, a choice was made in the presented case study to apply one single

640   average value for the substance removal efficiency across all wastewater facilities, including DWTS.

To evaluate the general performance of HydroFATE regarding its simulation of SMX concentrations, PECs resulting from the model were compared with MECs reported in the literature. The results showed an overall reasonable predictive capability

with 79% of PECs being within one order of magnitude of reported MECs. This was despite the inherent uncertainties associated with assumptions made in the development of the model and those associated with estimates of the various model

645 parameters and input datasets. Unfortunately, the lack of specificity of field measurements, for which literature sources generally do not provide enough information on the precise locations of measurements nor river discharge conditions, does not allow for a conclusive evaluation of the model under different modelling scenarios.

Importantly, the PECs simulated by the present version of HydroFATE are limited in that they do not include contaminant contributions from veterinary use or pharmaceutical manufacturing operations due to a lack of available data. As it remains

650 unclear whether MECs include SMX from only domestic or all sources, this uncertainty in both PECs and MECs could explain some of the high negative bias found in the evaluation. Once data on veterinary use or manufacturing become available, they could readily be implemented to refine HydroFATE.

6 Conclusion

Despite its current shortcomings and inherent uncertainties, HydroFATE is the most spatially detailed global CFM currently

655 available. It tracks multiple pathways of contaminants in the river and lake environment and has the potential to be used for any CEC of domestic use. In its current version, HydroFATE is expected to be particularly useful to identify specific areas in the river network where high concentrations of contaminants may be found. As such, potential applications include the support of decision-making in order to prioritize and focus resources, regarding: (1) locations that should be the subject of detailed field measurements and local environmental impact studies; (2) the creation of scenarios for policy-making and management

660 of water resources at regional or international scales; (3) the development of screening methods to inform new regulation or guidelines for the pharmaceutical industry with respect to establishing markets for their products and performing regulatory compliance tests to safeguard ecosystems and human health; (4) the development of new or updated treatment standards for contaminants of emerging concern, including the establishment of design specifications for wastewater treatment system in specific regions; and (5) the deployment of new treatment technologies.

665 **Code and data availability**

Model predictions for the four main scenarios were obtained with a run time of 18 min using a Desktop PC with Intel Core i7-10700 CPU 2.90 GHz and 32 GB RAM. The code for HydroFATE v1 (including compiling instructions) is available under the GNU General Public License v3.0 and the input and output data are available under a CC-BY-4.0 License at the following URL: https://doi.org/10.6084/m9.figshare.23646282. The global river network dataset and the associated attribute information

670 for every river reach as well as the results from the case study are also available at the same URL under the CC-BY-4.0 License.

Author contribution

Heloisa Ehalt Macedo: Conceptualization, Methodology, Software, Validation, Formal analysis, Investigation, Data Curation, Writing – Original Draft, Visualization. **Bernhard Lehner:** Conceptualization, Methodology, Resources, Writing – Review & Editing, Supervision, Funding acquisition. **Jim Nicell:** Conceptualization, Methodology, Resources, Writing – Review & Editing, Supervision, Funding acquisition. **Günther Grill:** Conceptualization & Methodology of original model, Software.

Competing interests

The authors declare that they have no known competing financial interests or personal relationships that could have appeared to influence the work reported in this paper.

Acknowledgements

We thank Eili Y. Klein from the Center for Disease Dynamics, Economics & Policy for providing the country-level averages of annual consumption per capita of SMX. We also thank Ranish Shakya for the contribution on early model development stages of HydroFATE. This research has been supported by the Natural Sciences and Engineering Research Council of Canada (NSERC Discovery grant no. RGPIN/04541-2019 and RGPIN/03792-2016) and the James McGill Chair program of McGill University.

References

Aldekoa, J., Marcé, R., and Francés, F.: Fate and Degradation of Emerging Contaminants in Rivers: Review of Existing Models, in: Emerging Contaminants in River Ecosystems: Occurrence and Effects Under Multiple Stress Conditions, edited by: Petrovic, M., Sabater, S., Elosegi, A., and Barceló, D., Springer International Publishing, Cham, 159-193, doi: 10.1007/698_2015_5017, 2016.

Aldekoa, J., Medici, C., Osorio, V., Pérez, S., Marcé, R., Barceló, D., and Francés, F.: Modelling the emerging pollutant diclofenac with the GREAT-ER model: Application to the Llobregat River Basin, Journal of Hazardous Materials, 263, 207-213, doi: 10.1016/j.jhazmat.2013.08.057, 2013.

Anderson, P. D., D'Aco, V. J., Shanahan, P., Chapra, S. C., Buzby, M. E., Cunningham, V. L., DuPlessie, B. M., Hayes, E. P., Mastrocco, F. J., Parke, N. J., Rader, J. C., Samuelian, J. H., and Schwab, B. W.: Screening Analysis of Human Pharmaceutical Compounds in U.S. Surface Waters, Environmental Science & Technology, 38, 838-849, doi: 10.1021/es034430b, 2004.

Archundia, D., Boithias, L., Duwig, C., Morel, M. C., Flores Aviles, G., and Martins, J. M. F.: Environmental fate and ecotoxicological risk of the antibiotic sulfamethoxazole across the Katari catchment (Bolivian Altiplano): Application of the GREAT-ER model, Science of The Total Environment, 622-623, 1046-1055, doi: 10.1016/j.scitotenv.2017.12.026, 2018.

700 Aydin, S., Aydin, M. E., Ulvi, A., and Kilic, H.: Antibiotics in hospital effluents: occurrence, contribution to urban wastewater, removal in a wastewater treatment plant, and environmental risk assessment, Environmental Science and Pollution Research, 26, 544-558, doi: 10.1007/s11356-018-3563-0, 2019.

aus der Beek, T., Weber, F. A., Bergmann, A., Hickmann, S., Ebert, I., Hein, A., and Küster, A.: Pharmaceuticals in the environment—Global occurrences and perspectives, Environmental Toxicology and Chemistry, 35, 823-835, doi: 705 10.1002/etc.3339, 2016.

Bengtsson-Palme, J. and Larsson, D. G. J.: Concentrations of antibiotics predicted to select for resistant bacteria: Proposed limits for environmental regulation, Environment International, 86, 140-149, doi: 10.1016/j.envint.2015.10.015, 2016.

Beusen, A. H. W., Van Beek, L. P. H., Bouwman, A. F., Mogollón, J. M., and Middelburg, J. J.: Coupling global models for hydrology and nutrient loading to simulate nitrogen and phosphorus retention in surface water – description of IMAGE– 710 GNM and analysis of performance, Geosci. Model Dev., 8, 4045-4067, doi: 10.5194/gmd-8-4045-2015, 2015.

Daughton, C. G.: The Matthew Effect and widely prescribed pharmaceuticals lacking environmental monitoring: Case study of an exposure-assessment vulnerability, Science of The Total Environment, 466-467, 315-325, doi: 10.1016/j.scitotenv.2013.06.111, 2014.

Daughton, C. G. and Ternes, T. A.: Pharmaceuticals and personal care products in the environment: agents of subtle change?, 715 Environ Health Perspect, 107 Suppl 6, 907-938, doi: 10.1289/ehp.99107s6907, 1999.

Ehalt Macedo, H., Lehner, B., Nicell, J., Grill, G.: HydroFATE version1, Figshare, doi: 10.6084/m9.figshare.23646282, 2023.

Ehalt Macedo, H., Lehner, B., Nicell, J., Grill, G., Li, J., Limtong, A., and Shakya, R.: Distribution and characteristics of wastewater treatment plants within the global river network, Earth Syst. Sci. Data, 14, 559-577, doi: 10.5194/essd-14-559-2022, 2022.

720 Feijtel, T., Boeije, G., Matthies, M., Young, A., Morris, G., Gandolfi, C., Hansen, B., Fox, K., Holt, M., Koch, V., Schroder, R., Cassani, G., Schowanek, D., Rosenblom, J., and Niessen, H.: Development of a geography-referenced regional exposure assessment tool for European rivers - great-er contribution to great-er #1, Chemosphere, 34, 2351-2373, doi: 10.1016/S0045-6535(97)00048-9, 1997.

Ferrari, B., Mons, R., Vollat, B., Fraysse, B., Paxēaus, N., Giudice, R. L., Pollio, A., and Garric, J.: Environmental risk 725 assessment of six human pharmaceuticals: Are the current environmental risk assessment procedures sufficient for the protection of the aquatic environment?, Environmental Toxicology and Chemistry, 23, 1344-1354, doi: 10.1897/03-246, 2004.

Font, C., Bregoli, F., Acuña, V., Sabater, S., and Marcé, R.: GLOBAL-FATE (version 1.0.0): A geographical information system (GIS)-based model for assessing contaminants fate in the global river network, Geosci. Model Dev., 12, 5213-5228, doi: 10.5194/gmd-12-5213-2019, 2019.

730   Gao, P., Ding, Y., Li, H., and Xagoraraki, I.: Occurrence of pharmaceuticals in a municipal wastewater treatment plant: mass balance and removal processes, Chemosphere, 88, 17-24, doi: 10.1016/j.chemosphere.2012.02.017, 2012.

Gavrilescu, M., Demnerová, K., Aamand, J., Agathos, S., and Fava, F.: Emerging pollutants in the environment: present and future challenges in biomonitoring, ecological risks and bioremediation, New Biotechnology, 32, 147-156, doi: 10.1016/j.nbt.2014.01.001, 2015.

735   Grill, G., Khan, U., Lehner, B., Nicell, J., and Ariwi, J.: Risk assessment of down-the-drain chemicals at large spatial scales: Model development and application to contaminants originating from urban areas in the Saint Lawrence River Basin, Science of The Total Environment, 541, 825-838, doi: 10.1016/j.scitotenv.2015.09.100, 2016.

Grill, G., Lehner, B., Thieme, M., Geenen, B., Tickner, D., Antonelli, F., Babu, S., Borrelli, P., Cheng, L., Crochetiere, H., Ehalt Macedo, H., Filgueiras, R., Goichot, M., Higgins, J., Hogan, Z., Lip, B., McClain, M. E., Meng, J., Mulligan, M., Nilsson,
740   C., Olden, J. D., Opperman, J. J., Petry, P., Reidy Liermann, C., Sáenz, L., Salinas-Rodríguez, S., Schelle, P., Schmitt, R. J. P., Snider, J., Tan, F., Tockner, K., Valdujo, P. H., van Soesbergen, A., and Zarfl, C.: Mapping the world's free-flowing rivers, Nature, 569, 215-221, doi: 10.1038/s41586-019-1111-9, 2019.

Grill, G., Li, J., Khan, U., Zhong, Y., Lehner, B., Nicell, J., and Ariwi, J.: Estimating the eco-toxicological risk of estrogens in China's rivers using a high-resolution contaminant fate model, Water Research, 145, 707-720, doi:
745   10.1016/j.watres.2018.08.053, 2018.

Grill, G., Ouellet Dallaire, C., Fluet Chouinard, E., Sindorf, N., and Lehner, B.: Development of new indicators to evaluate river fragmentation and flow regulation at large scales: A case study for the Mekong River Basin, Ecological Indicators, 45, 148-159, doi: 10.1016/j.ecolind.2014.03.026, 2014.

Gupta, H. V., Kling, H., Yilmaz, K. K., and Martinez, G. F.: Decomposition of the mean squared error and NSE performance
750   criteria: Implications for improving hydrological modelling, Journal of Hydrology, 377, 80-91, doi: 10.1016/j.jhydrol.2009.08.003, 2009.

Hanna, N., Purohit, M., Diwan, V., Chandran, S. P., Riggi, E., Parashar, V., Tamhankar, A. J., and Lundborg, C. S.: Monitoring of Water Quality, Antibiotic Residues, and Antibiotic-Resistant Escherichia coli in the Kshipra River in India over a 3-Year Period, Int J Environ Res Public Health, 17, doi: 10.3390/ijerph17217706, 2020.

755   Havnø, K., Madsen, M., and Dørge, J.: MIKE 11–a generalized river modelling package, in: Computer models of watershed hydrology, Water Resources Publications, Colorado, USA, 733-782, 1995.

Hernando, M. D., Mezcua, M., Fernández-Alba, A. R., and Barceló, D.: Environmental risk assessment of pharmaceutical residues in wastewater effluents, surface waters and sediments, Talanta, 69, 334-342, doi: 10.1016/j.talanta.2005.09.037, 2006.

760   Herrera, V.: Reconciling global aspirations and local realities: Challenges facing the Sustainable Development Goals for water and sanitation, World Development, 118, 106-117, doi: 10.1016/j.worlddev.2019.02.009, 2019.

Hofstra, N., Bouwman, A. F., Beusen, A. H. W., and Medema, G. J.: Exploring global Cryptosporidium emissions to surface water, Science of The Total Environment, 442, 10-19, doi: 10.1016/j.scitotenv.2012.10.013, 2013.

Johnson, A. C., Dumont, E., Williams, R. J., Oldenkamp, R., Cisowska, I., and Sumpter, J. P.: Do Concentrations of Ethinylestradiol, Estradiol, and Diclofenac in European Rivers Exceed Proposed EU Environmental Quality Standards?,
765   Environmental Science & Technology, 47, 12297-12304, doi: 10.1021/es4030035, 2013.

Johnson, A. C., Keller, V., Williams, R. J., and Young, A.: A practical demonstration in modelling diclofenac and propranolol river water concentrations using a GIS hydrology model in a rural UK catchment, Environmental Pollution, 146, 155-165, doi: 10.1016/j.envpol.2006.05.037, 2007.

Johnson, A. C., Ternes, T., Williams, R. J., and Sumpter, J. P.: Assessing the Concentrations of Polar Organic
770   Microcontaminants from Point Sources in the Aquatic Environment: Measure or Model?, Environmental Science & Technology, 42, 5390-5399, doi: 10.1021/es703091r, 2008.

K'Oreje, K. O., Demeestere, K., De Wispelaere, P., Vergeynst, L., Dewulf, J., and Van Langenhove, H.: From multi-residue screening to target analysis of pharmaceuticals in water: Development of a new approach based on magnetic sector mass spectrometry and application in the Nairobi River basin, Kenya, Science of The Total Environment, 437, 153-164, doi:
775   10.1016/j.scitotenv.2012.07.052, 2012.

Kapo, K. E., Paschka, M., Vamshi, R., Sebasky, M., and McDonough, K.: Estimation of U.S. sewer residence time distributions for national-scale risk assessment of down-the-drain chemicals, Science of The Total Environment, 603-604, 445-452, doi: 10.1016/j.scitotenv.2017.06.075, 2017.

Keller, V., Fox, K., Rees, H. G., and Young, A. R.: Estimating population served by sewage treatment works from readily
780   available GIS data, Science of The Total Environment, 360, 319-327, doi: 10.1016/j.scitotenv.2005.08.043, 2006.

Khan, G. A., Berglund, B., Khan, K. M., Lindgren, P.-E., and Fick, J.: Occurrence and abundance of antibiotics and resistance genes in rivers, canal and near drug formulation facilities–a study in Pakistan, PloS one, 8, e62712, doi: 10.1371/journal.pone.0062712, 2013.

Klein, E. Y., Boeckel, T. P. V., Martinez, E. M., Pant, S., Gandra, S., Levin, S. A., Goossens, H., and Laxminarayan, R.:
785   Global increase and geographic convergence in antibiotic consumption between 2000 and 2015, Proceedings of the National Academy of Sciences, 115, E3463-E3470, doi: 10.1073/pnas.1717295115, 2018.

Kroeze, C., Gabbert, S., Hofstra, N., Koelmans, A. A., Li, A., Löhr, A., Ludwig, F., Strokal, M., Verburg, C., Vermeulen, L., van Vliet, M. T. H., de Vries, W., Wang, M., and van Wijnen, J.: Global modelling of surface water quality: a multi-pollutant approach, Current Opinion in Environmental Sustainability, 23, 35-45, doi: 10.1016/j.cosust.2016.11.014, 2016.

790 Kümmerer, K.: The presence of pharmaceuticals in the environment due to human use – present knowledge and future challenges, Journal of Environmental Management, 90, 2354-2366, doi: 10.1016/j.jenvman.2009.01.023, 2009.

Lam, Q. D., Schmalz, B., and Fohrer, N.: Modelling point and diffuse source pollution of nitrate in a rural lowland catchment using the SWAT model, Agricultural Water Management, 97, 317-325, doi: 10.1016/j.agwat.2009.10.004, 2010.

Lapworth, D. J., Baran, N., Stuart, M. E., and Ward, R. S.: Emerging organic contaminants in groundwater: A review of 795 sources, fate and occurrence, Environmental Pollution, 163, 287-303, doi: 10.1016/j.envpol.2011.12.034, 2012.

Lehner, B. and Grill, G.: Global river hydrography and network routing: baseline data and new approaches to study the world's large river systems, Hydrol Process, 27, 2171-2186, doi: 10.1002/hyp.9740, 2013.

Lehner, B., Verdin, K., and Jarvis, A.: New global hydrography derived from spaceborne elevation data, Eos, 89, 93-94, doi: 10.1029/2008EO100001, 2008.

800 Linke, S., Lehner, B., Ouellet Dallaire, C., Ariwi, J., Grill, G., Anand, M., Beames, P., Burchard-Levine, V., Maxwell, S., Moidu, H., Tan, F., and Thieme, M.: Global hydro-environmental sub-basin and river reach characteristics at high spatial resolution, Scientific Data, 6, 283, doi: 10.1038/s41597-019-0300-6, 2019.

Mackay, D., Di Guardo, A., Paterson, S., Kicsi, G., Cowan, C. E., and Kane, D. M.: Assessment of chemical fate in the environment using evaluative, regional and local-scale models: Illustrative application to chlorobenzene and linear 805 alkylbenzene sulfonates, Environmental Toxicology and Chemistry, 15, 1638-1648, doi: 10.1002/etc.5620150930, 1996.

Mayorga, E., Seitzinger, S. P., Harrison, J. A., Dumont, E., Beusen, A. H. W., Bouwman, A. F., Fekete, B. M., Kroeze, C., and Van Drecht, G.: Global Nutrient Export from WaterSheds 2 (NEWS 2): Model development and implementation, Environmental Modelling & Software, 25, 837-853, doi: 10.1016/j.envsoft.2010.01.007, 2010.

Messager, M. L., Lehner, B., Grill, G., Nedeva, I., and Schmitt, O.: Estimating the volume and age of water stored in global 810 lakes using a geo-statistical approach, Nature Communications, 7, 13603, doi: 10.1038/ncomms13603, 2016.

Meyer, M. F., Powers, S. M., and Hampton, S. E.: An Evidence Synthesis of Pharmaceuticals and Personal Care Products (PPCPs) in the Environment: Imbalances among Compounds, Sewage Treatment Techniques, and Ecosystem Types, Environmental Science & Technology, 53, 12961-12973, doi: 10.1021/acs.est.9b02966, 2019.

Müller Schmied, H., Eisner, S., Franz, D., Wattenbach, M., Portmann, F. T., Flörke, M., and Döll, P.: Sensitivity of simulated 815 global-scale freshwater fluxes and storages to input data, hydrological model structure, human water use and calibration, Hydrol. Earth Syst. Sci., 18, 3511-3538, doi: 10.5194/hess-18-3511-2014, 2014.

Nash, J. E. and Sutcliffe, J. V.: River flow forecasting through conceptual models part I—A discussion of principles, Journal of hydrology, 10, 282-290, 1970.

Noguera-Oviedo, K. and Aga, D. S.: Lessons learned from more than two decades of research on emerging contaminants in the environment, Journal of Hazardous Materials, 316, 242-251, doi: 10.1016/j.jhazmat.2016.04.058, 2016.

Oldenkamp, R., Hoeks, S., Čengić, M., Barbarossa, V., Burns, E. E., Boxall, A. B. A., and Ragas, A. M. J.: A High-Resolution Spatial Model to Predict Exposure to Pharmaceuticals in European Surface Waters: ePiE, Environmental Science & Technology, 52, 12494-12503, doi: 10.1021/acs.est.8b03862, 2018.

Palli, L., Spina, F., Varese, G. C., Vincenzi, M., Aragno, M., Arcangeli, G., Mucci, N., Santianni, D., Caffaz, S., and Gori, R.: Occurrence of selected pharmaceuticals in wastewater treatment plants of Tuscany: An effect-based approach to evaluate the potential environmental impact, International Journal of Hygiene and Environmental Health, 222, 717-725, doi: 10.1016/j.ijheh.2019.05.006, 2019.

Patrolecco, L., Rauseo, J., Ademollo, N., Grenni, P., Cardoni, M., Levantesi, C., Luprano, M. L., and Caracciolo, A. B.: Persistence of the antibiotic sulfamethoxazole in river water alone or in the co-presence of ciprofloxacin, Science of The Total Environment, 640-641, 1438-1446, doi: 10.1016/j.scitotenv.2018.06.025, 2018.

Petrie, B., Barden, R., and Kasprzyk-Hordern, B.: A review on emerging contaminants in wastewaters and the environment: Current knowledge, understudied areas and recommendations for future monitoring, Water Research, 72, 3-27, doi: 10.1016/j.watres.2014.08.053, 2015.

Pistocchi, A., Sarigiannis, D. A., and Vizcaino, P.: Spatially explicit multimedia fate models for pollutants in Europe: State of the art and perspectives, Science of The Total Environment, 408, 3817-3830, doi: 10.1016/j.scitotenv.2009.10.046, 2010.

Praveena, S. M., Shaifuddin, S. N. M., Sukiman, S., Nasir, F. A. M., Hanafi, Z., Kamarudin, N., Ismail, T. H. T., and Aris, A. Z.: Pharmaceuticals residues in selected tropical surface water bodies from Selangor (Malaysia): Occurrence and potential risk assessments, Science of The Total Environment, 642, 230-240, doi: 10.1016/j.scitotenv.2018.06.058, 2018.

Rizzo, L., Malato, S., Antakyali, D., Beretsou, V. G., Đolić, M. B., Gernjak, W., Heath, E., Ivancev-Tumbas, I., Karaolia, P., Lado Ribeiro, A. R., Mascolo, G., McArdell, C. S., Schaar, H., Silva, A. M. T., and Fatta-Kassinos, D.: Consolidated vs new advanced treatment methods for the removal of contaminants of emerging concern from urban wastewater, Science of The Total Environment, 655, 986-1008, doi: 10.1016/j.scitotenv.2018.11.265, 2019.

Rudy, B. C. and Senkowski, B. Z.: Sulfamethoxazole, in: Analytical Profiles of Drug Substances, edited by: Florey, K., Academic Press, 467-486, doi: 10.1016/S0099-5428(08)60051-9, 1973.

Schneider, A., Friedl, M. A., and Potere, D.: Mapping global urban areas using MODIS 500-m data: New methods and datasets based on 'urban ecoregions', Remote Sensing of Environment, 114, 1733-1746, doi: 10.1016/j.rse.2010.03.003, 2010.

Shakya, R. M.: Prediction of household pharmaceutical concentrations in rivers of the Indian subcontinent using a contaminant fate model, Department of Geography, McGill University, https://escholarship.mcgill.ca/concern/theses/x920g017b, 2017.

Sridhar, K. S. and Mavrotas, G.: Challenges of urbanization in the global south: Introduction and overview, in: Urbanization
850   in the Global South, Routledge India, 1-17, doi: 10.4324/9781003093282-1, 2021.

Straub, J. O.: Aquatic environmental risk assessment for human use of the old antibiotic sulfamethoxazole in Europe, Environ Toxicol Chem, 35, 767-779, doi: 10.1002/etc.2945, 2016.

Strokal, M., Spanier, J. E., Kroeze, C., Koelmans, A. A., Flörke, M., Franssen, W., Hofstra, N., Langan, S., Tang, T., van Vliet, M. T. H., Wada, Y., Wang, M., van Wijnen, J., and Williams, R.: Global multi-pollutant modelling of water quality: scientific
855   challenges and future directions, Current Opinion in Environmental Sustainability, 36, 116-125, doi: 10.1016/j.cosust.2018.11.004, 2019.

Tang, T., Strokal, M., van Vliet, M. T. H., Seuntjens, P., Burek, P., Kroeze, C., Langan, S., and Wada, Y.: Bridging global, basin and local-scale water quality modeling towards enhancing water quality management worldwide, Current Opinion in Environmental Sustainability, 36, 39-48, doi: 10.1016/j.cosust.2018.10.004, 2019.

860   Tatem, A. J.: WorldPop, open data for spatial demography, Scientific Data, 4, 170004, doi: 10.1038/sdata.2017.4, 2017.

Van Drecht, G., Bouwman, A. F., Harrison, J., and Knoop, J. M.: Global nitrogen and phosphate in urban wastewater for the period 1970 to 2050, Global Biogeochemical Cycles, 23, doi: 10.1029/2009gb003458, 2009.

van Puijenbroek, P. J. T. M., Beusen, A. H. W., and Bouwman, A. F.: Global nitrogen and phosphorus in urban waste water based on the Shared Socio-economic pathways, Journal of Environmental Management, 231, 446-456, doi:
865   10.1016/j.jenvman.2018.10.048, 2019.

van Vliet, M. T. H., Flörke, M., Harrison, J. A., Hofstra, N., Keller, V., Ludwig, F., Spanier, J. E., Strokal, M., Wada, Y., Wen, Y., and Williams, R. J.: Model inter-comparison design for large-scale water quality models, Current Opinion in Environmental Sustainability, 36, 59-67, doi: 10.1016/j.cosust.2018.10.013, 2019.

van Wijnen, J., Ragas, A. M. J., and Kroeze, C.: River export of triclosan from land to sea: A global modelling approach,
870   Science of The Total Environment, 621, 1280-1288, doi: 10.1016/j.scitotenv.2017.10.100, 2018.

Vermeire, T., Rikken, M., Attias, L., Boccardi, P., Boeije, G., Brooke, D., de Bruijn, J., Comber, M., Dolan, B., Fischer, S., Heinemeyer, G., Koch, V., Lijzen, J., Müller, B., Murray-Smith, R., and Tadeo, J.: European union system for the evaluation of substances: the second version, Chemosphere, 59, 473-485, doi: 10.1016/j.chemosphere.2005.01.062, 2005.

Voß, A., Alcamo, J., Bärlund, I., Voß, F., Kynast, E., Williams, R., and Malve, O.: Continental scale modelling of in-stream
875   river water quality: a report on methodology, test runs, and scenario application, Hydrol Process, 26, 2370-2384, doi: 10.1002/hyp.9445, 2012.

Wang, X., Hao, F., Cheng, H., Yang, S., Zhang, X., and Bu, Q.: Estimating non-point source pollutant loads for the large-scale basin of the Yangtze River in China, Environmental Earth Sciences, 63, 1079-1092, doi: 10.1007/s12665-010-0783-0, 2011.

Wang, X., White-Hull, C., Dyer, S., and Yang, Y.: GIS-ROUT: A River Model for Watershed Planning, Environment and Planning B: Planning and Design, 27, 231-246, doi: 10.1068/b2624, 2000.

Wilkinson, J. L., Boxall, A. B. A., Kolpin, D. W., Leung, K. M. Y., Lai, R. W. S., Galbán-Malagón, C., Adell, A. D., Mondon, J., Metian, M., Marchant, R. A., Bouzas-Monroy, A., Cuni-Sanchez, A., Coors, A., Carriquiriborde, P., Rojo, M., Gordon, C., Cara, M., Moermond, M., Luarte, T., . . . Teta, C. Pharmaceutical pollution of the world's rivers. Proceedings of the National Academy of Sciences, 119(8), e2113947119. doi:10.1073/pnas.2113947119, 2022

Williams, R., Keller, V., Voß, A., Bärlund, I., Malve, O., Riihimäki, J., Tattari, S., and Alcamo, J.: Assessment of current water pollution loads in Europe: estimation of gridded loads for use in global water quality models, Hydrol Process, 26, 2395-2410, doi: 10.1002/hyp.9427, 2012.

World Bank. GNI per capita, Atlas method. Retrieved December 2019 from https://datahelpdesk.worldbank.org/knowledgebase/articles/906519-world-bank-country-and-lending-groups., 2019.

World Health Organization (WHO), & United Nations International Children's Emergency Fund.(UNICEF). Joint Monitoring Programme (JMP) for water supply and sanitation. Retrieved December 2019 from https://washdata.org/, 2021

WorldPop, & Center for International Earth Science Information Network. Global High Resolution Population Denominators Project (The Bill and Melinda Gates Foundation, Trans.). Columbia University, 2018.

Yadav, D., Rangabhashiyam, S., Verma, P., Singh, P., Devi, P., Kumar, P., Hussain, C. M., Gaurav, G. K., and Kumar, K. S.: Environmental and health impacts of contaminants of emerging concerns: Recent treatment challenges and approaches, Chemosphere, 272, 129492, doi: 10.1016/j.chemosphere.2020.129492, 2021.

Yuan, D., Lin, B., Falconer, R. A., and Tao, J.: Development of an integrated model for assessing the impact of diffuse and point source pollution on coastal waters, Environmental Modelling & Software, 22, 871-879, doi: 10.1016/j.envsoft.2006.05.010, 2007.

Zhang, Z. and Tang, W.: Drug metabolism in drug discovery and development, Acta Pharm Sin B, 8, 721-732, doi: 10.1016/j.apsb.2018.04.003, 2018.